2012•2013
FACULTEIT GENEESKUNDE EN LEVENSWETENSCHAPPEN
master in de biomedische wetenschappen: bio-elektronica en nanotechnologie

Masterproef

Heat-transfer resistance based biosensor to detect mutation in patients with PKU

Promotor :
dr. Veronique VERMEEREN

Heman Kumar Ramiya Ramesh Babu

Masterproef voorgedragen tot het bekomen van de graad van master in de biomedische wetenschappen , afstudeerrichting bio-elektronica en nanotechnologie

De transnationale Universiteit Limburg is een uniek samenwerkingsverband van twee universiteiten in twee landen: de Universiteit Hasselt en Maastricht University.

universiteit hasselt
KNOWLEDGE IN ACTION
Universiteit Hasselt | Campus Hasselt | Martelarenlaan 42 | BE-3500 Hasselt
Universiteit Hasselt | Campus Diepenbeek | Agoralaan Gebouw D | BE-3590 Diepenbeek

universiteit hasselt | Maastricht University

2012•2013
FACULTEIT GENEESKUNDE EN LEVENSWETENSCHAPPEN
master in de biomedische wetenschappen: bio-elektronica en nanotechnologie

Masterproef

Heat-transfer resistance based biosensor to detect mutation in patients with PKU

Promotor :
dr. Veronique VERMEEREN

Heman Kumar Ramiya Ramesh Babu
Masterproef voorgedragen tot het bekomen van de graad van master in de biomedische wetenschappen , afstudeerrichting bio-elektronica en nanotechnologie

universiteit hasselt | Maastricht University

Preface

∞ Thanks to the one, who drew'st, and mad'st me to complete this piece of work Ω

All the work presented in this thesis was conducted at the Biomedical Research Institute of Hasselt University, Campus Diepenbeek, Agoralaan Building C, BE 3590.

I take immense pleasure in thanking Prof. Dr. Luc Michiels and Dr. Veronique Vermeeren for giving me this great opportunity to carry out my master dissertation in their group.

Thanks to Dra. Natalie Vanden Bon for introducing me to the various techniques and motivating me to carry out different experiments.

Thanks to Miss Lotte Vanbrabant and Ms. Igna Rutten for helping me to find the correct protocols and for making orders on time.

Thanks to Dra. Katrijn Vanschoenbeek, Drs. Kaushik Rajaram and Drs. Jeroen Vanbrabant for the support during Natalie's absence.

Special thanks to Dr. Veronique Vermeeren for revising and perfecting this very thesis into a piece of significant scientific literature.

Finally, thanks to my family for letting me pursue my selfish dreams.

Table of Contents

List of abbreviations

- A U : arbitrary units
- B : bases
- BH_4 : tetrahydrobiopterin
- bp : basepairs
- CVD : chemical vapour deposition
- DGGE : denaturing gradient gel electrophoresis
- DNA : deoxyribonucleic acid
- dsDNA : doublestranded deoxyribonucleic acid
- EDC : 1-ethyl-3-(3-dimethylaminopropyl)carbodiimide
- EIS : electrochemical impedance spectroscopy
- FITC : fluorescein isothiocyanate
- MES : 2-(N-morpholino)ethanesulfonic acid
- NCD : nanocrystalline diamond
- P : power
- PAH : phenylalanine hydroxylase
- PBS : phosphate buffered saline
- PCR : polymerase chain reaction
- PKU : Phenylketonuria
- QCM : Quartz crystal microbalance
- R : resistance
- R.U : resonance unit
- RBC : red blood cells
- Rth : heat transfer resistance
- SDS : odium dodecyl sulphate
- SNP : singe nucleotide polymorphism
- SPR : surface plasmon resonance
- SSC : saline-sodium citrate (SSC) buffer
- ssDNA-singlestranded deoxyribonucleic acid
- T : temperature
- *Taq* : *Thermas aquaticus*
- V : voltage

Abstract

Purpose: This study was intended to develop a label-free, simple sensing platform that can detect SNPs in the exons of the PAH gene based on heat transfer resistance (Rth). This technique was developed with short DNA strands by van Grinsven *et al.*, 2012. The objective of this study was to extend this principle towards exon-size DNA fragments to simplify gene-screening arrays. A main focus point was to determine the maximum length of DNA that can still be employed for this Rth platform.

Subjects and Methods: The immobilization efficiency of longer DNA was determined with confocal fluorescence microscopy by analysing the NCD, to which probe ssDNA of different lengths were attached and hybridized with detection probes labelled with Alexa Fluor® 488. Following this, the suitability of these long strands for Rth measurements was checked by attaching synthetic probe strands encompassing the sequence of 4 PAH gene exons: 5 (98 bp), 7 (150 bp), 9 (66 bp), and 12 (123 bp), and hybridizing them to their synthetic wildtype targets, forming homoduplexes, and to targets containing a SNP, forming heteroduplexes. Rth was monitored during the denaturation and the difference in Rth behaviour was evaluated for both of these duplexes. Based on the maximum DNA length that was thus found to still be suitable for Rth measurements, the 12 exons of the PAH gene were analysed and exons that were longer than the optimal length were divided into two overlapping sequences (exon 3 and 6) to function as attachment probes. To isolate the exon fragments from real donor samples in order to generate target material for hybridization to the Rth sensor, 14 primers pairs were designed and optimized to yield amplicons that were converted to ssDNA through Lambda Exonuclease digestion. Finally, Rth was evaluated during the denaturation of homoduplexes formed with real donor target ssDNA of exon 5 generated in the above described way.

Results: The confocal microscopy results indicated that immobilization was still efficient at 200 b, allowing the covalent attachment of all PAH exons. The Rth study with synthetic probe and target strands suggested that the DNA length limit that still allows discrimination between wildtype and SNP, is somewhere between 123 and 150 bp. We were able to detect prevalent mutations in exon 5 (c.473 G>C), exon 9 (c.932 T>C) and exon 12 (c.124 G>C). The homo- and heteroduplexes of exons that were less than 100 bp (exon 5 and 9) were easy to discriminate with Rth. However, it became difficult as the length increased to more than 100 b (exon 12). Duplexes that were around 150 b (exon 7) showed an Rth shift that were random for homo- and heteroduplexes. This is due to the fact that approaching the persistence length of dsDNA decreases the resolution between ssDNA and dsDNA. We observed a biphasal Rth shift when the homoduplex formed with target DNA that was generated from a healthy donor was subjected to Rth measurements. This is as yet not completely understood.

Conclusion: This study proves that longer fragments of up to at least 123 b can be employed for detecting SNPs with this Rth platform, with real donor DNA material.

Introduction

Phenylketonuria (PKU) is a metabolic, genetic disorder caused by mutations in the PAH gene that encodes the enzyme phenylalanine hydroxylase (PAH). This hepatic enzyme converts the amino acid phenylalanine into the amino acid tyrosine in the presence of oxygen and tetrahydrobiopterin (BH_4). When it fails to metabolize, phenylalanine accumulates and results in a medical condition called hyperphenylalaninemia (HPA), which has a neurotoxic effect [1]. Undiagnosed individuals will show several cognitive dysfunctions such as abnormal behaviour, hyperactivity and schizophrenic signs.

PKU is a recessively inheritable disease, which is found in individuals who are homozygous for a mutation in the PAH gene. It is inherited with a chance of one in four children when both parents carry a mutation in only one PAH gene. In addition to the 98% of PKU cases that are caused by a mutation in both PAH genes, the remaining 2% of the cases is due to BH_4 deficiency.

The neurotoxic effects can be arrested easily when the patients are diagnosed in the early stages of the disease and maintain a strict low-phenylalanine diet. Hence, PKU screening is made mandatory for newborns in most countries. The screening is done by determining the amount of phenylalanine and tyrosine in the blood of the newborn [2]. However, diagnosis through biochemical methods is only concerned with the phenotype resulting from the mutation. It fails to discriminate the genetic trait, whether the individual is homozygous or heterozygous for the trait, or whether the patient suffers from classical PKU or from BH_4-deficient HPA. Hence, there is a need for a diagnosis through a genetic test, which would provide sufficient information about the mutation in the PAH genes of the individual. More than 560 mutations were reported in the PAH gene and some of the mutations occur at the splice junction sites between introns and exons. Traditional analytical methods that are based on genetic tests include denaturing gradient gel electrophoresis (DGGE) and direct sequencing of the gene through the Sanger method [1]. DNA sequencing is a routine, widespread technique that is being used for genome analysis and mutation detection. In sequencing, the target sequences are amplified by PCR and sequenced through the incorporation of fluorescently labelled nucleotides. However, *Taq* DNA polymerase, the most commonly used enzyme, might lead to errors at a rate of 10^{-4} to 10^{-5} per nucleotide. To avoid this, high fidelity DNA polymerases are employed. This method is efficient for studying mutations but it is time consuming and expensive. In addition to the automated Sanger sequencing, which can generate only 96 kb sequences per run, next generation sequencing methods such as Illumina/Solexa and ABI/SOLiD can generate up to 1-3 Gb sequences per run. The growing advancements in the sequencing technology towards reducing the time and cost is discussed elsewhere [17, 18]. In DGGE, sequences with and without a mutation can be resolved into unique band patterns in a denaturing polyacrylamide gel, based on decreased electrophoretic mobility of denatured DNA [3]. The presence of mutations will yield sequences with lower melting temperatures as compared to those of the wildtype sequences, so they will denature sooner in the gel, creating the unique band patterns. Mutations are detected by DGGE using PCR products of the PAH gene fragment [4]. It can detect 50% of the sequence variants in the DNA fragments containing up to 500 bp and the percentage can be improved up to 100% by attaching a GC-clamp at the terminal ends of the fragment or a chemi-clamp at the 5'-end [5]. However, drawbacks of this technique are the requirement of expensive instrumentation and the fact that it is less suitable for parallelized analysis and high throughput. In an actual clinical situation DGGE is usually followed by direct sequencing for conformation reasons. Therefore, there is a need for a method that would allow straightforward, simple, fast and cost-effective genetic diagnosis of PKU.

Efforts have been made to circumvent the limitations imposed by the traditional methods for detecting mutations in PKU and other genetic disorders. In addition to DGGE and direct sequence analysis, various other DNA-based diagnostics, such as microarrays and DNA-sensors, have been developed.

These techniques exploit the hybridizing and denaturing properties of DNA double helices for mutation detection. DNA microarrays, for instance, are used in gene expression profiling, mutation analysis, and diagnosing several bacterial infections. It was first used in 1993 for diagnosing Hantavirus-associated respiratory disease. When using this technique for mutation analysis, probe DNA (i.e., a single-stranded (ss) DNA fragment corresponding to the genetic region under investigation) is immobilized on a glass substrate with a density of ~10,000/cm^2. Each probe represents a mutant variant of a gene. Target DNA (i.e. specimen DNA originating form a patient or healthy control), usually labelled with a fluorescent agent, and is added to the probe DNA. If the target DNA is complementary to the probe DNA they will hybridize by forming hydrogen bonds. About four hours after addition of the target DNA the un-hybridized or non-specifically bound target DNA is washed away. The intensity of the labels present on the chip is monitored and correlated to the probe DNA. If the probe DNA on the location of the hybridized spot represents a specific mutation known to be correlated with a disease, this mutation is present in the DNA sample. The immobilization methods and the applications of microarray technology are discussed elsewhere [6]. Despite the numerous applications and the advantages of this technology, they do have several disadvantages, like low sensitivity, high cost and technical requirements, the need for labelling, long incubation times and a rather high chance of false negative results. DNA-sensors are devices that also work based on sequence-specific recognition of DNA strands. Unlike microarrays, in a DNA-sensor the data acquisition occurs through various other readout methods than being based on optics (fluorescence). Electrochemistry (amperometry, conductometry, impedimetry, and field-effect), mass (surface plasmon resonance, SPR) and piezoelectricity (quartz crystal microbalance, QCM) are also popular readout techniques for DNA-sensors. Surface plasmon field-enhanced fluorescence spectroscopy (SPFS) is a relatively new technique that combines SPR and fluorescence spectroscopy to monitor the hybridization process and detect PCR products [6, 7, 8]. SPFS is highly sensitive and has a detection limit of 500 fmol. However, it still requires labelling and sophisticated instrumentation. Electrochemical DNA-sensors sense the electrochemical changes that occur in the recognition layer during hybridization and denaturation. For example, in one approach ssDNA was attached to a glassy carbon electrode as a probe and the target ssDNA was added to react. Then, the redox indicator Co (phen)$^{3+}$, which has an affinity for dsDNA, was added to obtain an electrochemical response. If the complementary target DNA is hybridized to the probe DNA, then a greater electrochemical response is obtained, and if not, because of the presence of mutations in the target DNA, the response is not significant. There are many other formats developed based on this technique [9, 10, and 11], which is highly sensitive, low-cost, requires low power and simple instrumentation. The detection limit that can be achieved through this method is in the femtomolar range [12]. However, this technique obligates the use of redox indicators and it does not work with longer fragments of DNA [13]. Wang *et al.* have demonstrated a label-free electrochemical method that uses the oxidation of guanine or iosine bases as a DNA sensing basis. In this method, the hybridization of guanine bases is detected by constant current chronopotentiometry, where the oxidation signal of guanine is well separated from that of iosine, and higher in dsDNA as compared to ssDNA [14]. The detection limit of this method is below 100 nM. However, it is limited to short sequences of 19 bases with at least 4 guanine bases [15]. Overall, the electrochemical methods risk causing irreversible damage to the immobilized DNA, making it impossible to reuse [15].

Impedimetric biosensors are another class of biosensors that employ electrochemical impedance spectroscopy (EIS) to probe the changes that occur in the transducer surface. EIS involves measuring the impedance between two electrodes, one of which is functionalized with DNA, at frequencies from 100 Hz to 10^6 Hz. In that category, Vermeeren *et al*., have demonstrated that single nucleotide polymorphism (SNP) detection can be performed in real-time, during hybridization and denaturation of homo- and heteroduplexes using EIS. In this method ssDNA was attached covalently to nanocrystalline diamond (NCD) via EDC coupling as reported [19]. At lower frequencies there was a decline in the

impedance during hybridization of the probe DNA with a complementary sequence, forming a homoduplex, and there was no significant impedance change when being hybridized with a sequence containing a mutation, forming a heteroduplex. Moreover, at higher frequencies, there was also a significant difference in the speed of the impedance decrease, but now during denaturation of homoduplexes and heteroduplexes with NaOH. The denaturation of heteroduplexes occurred faster than that of homoduplexes, because of the intrinsic instability of heteroduplexes. In subsequent report, Vermeeren *et al*. further studied the SNP sensitivity of heteroduplex denaturation by EIS. This employed an impedimetric flow cell in which the DNA was covalently attached on to NCD as mentioned above and denaturation was carried out by NaOH. Again, the homoduplexes had a longer denaturation time constant than the heteroduplexes. Despite various advantages of the EIS-based sensing, it involves complex calculations and switching of buffers, making it complicated.

Recently, van Grinsven *et al.* developed a method to study denaturation using heat, to circumvent the issue of buffer switching. They studied the temperature-dependent heat transfer property of DNA attached to an NCD substrate and found that ssDNA showed a high resistance to heat transfer (Rth) compared to dsDNA. The reason for this Rth difference is not clear yet, but one hypothesis is that this property arises because ssDNA attached to a substrate takes up the conformation of a ball-like structure, as shown in left of figure 1, insulating the surface, and thus hindering heat transfer. In contrast, dsDNA attached to a surface forms stiff rod-like structures, as shown in the right panel of figure 1, leaving space for heat transfer.

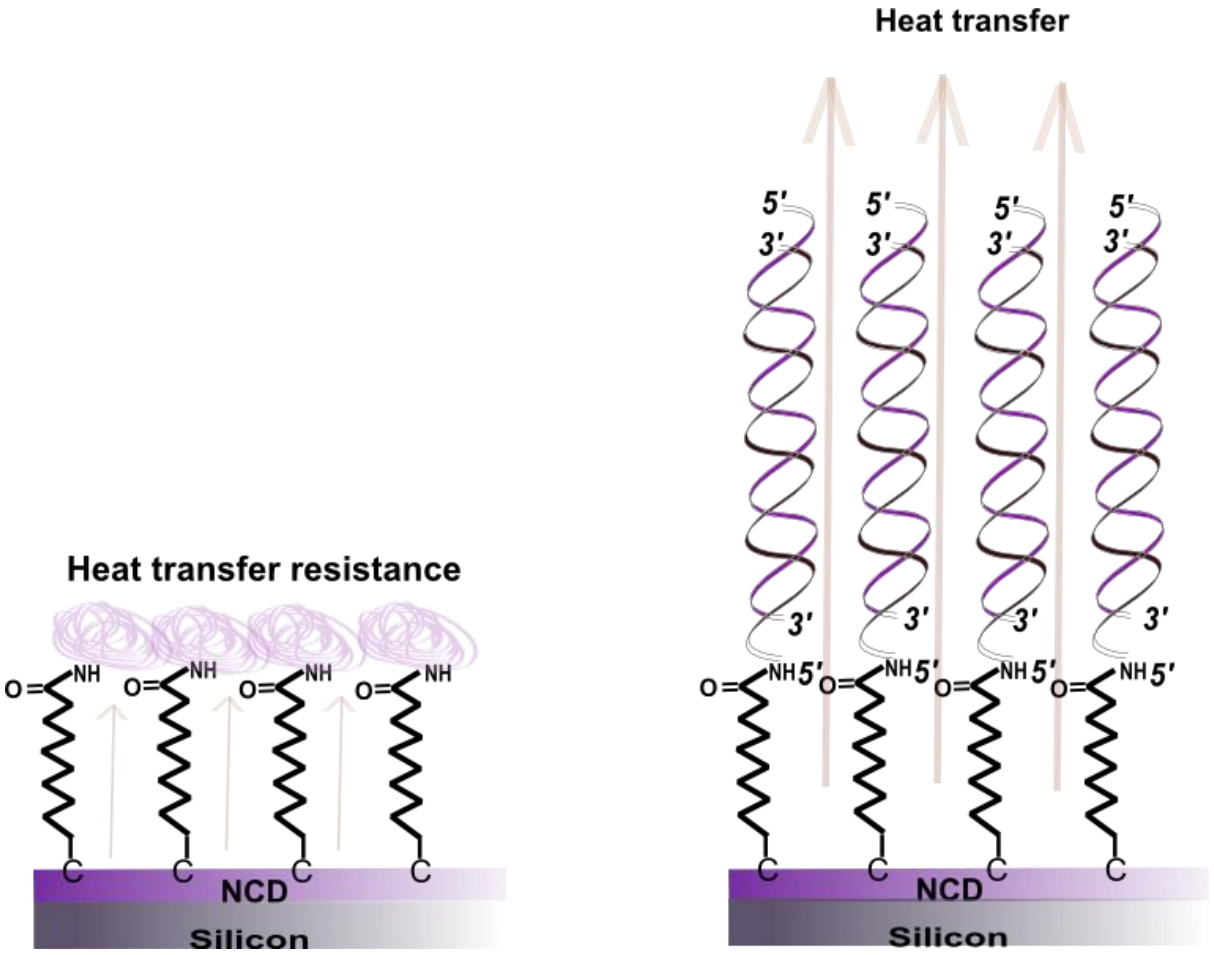

Figure 1. Structural morphology of ssDNA and dsDNA attached to a diamond substrate, and its effect on the efficiency of heat transfer.

Van Grinsven *et al.*, proved that this principle could be exploited for mutation detection during DNA denaturation. NCD samples were functionalized with ssDNA probes and hybridized with three types of target DNA: DNA that was completely complementary to the probe DNA, forming a homoduplex, DNA having a mismatch at the 7th base of the probe counting from the 3' terminus, and DNA having a mismatch at 20th base of the probe counting form its 3' terminus, both forming heteroduplexes. When subjected to thermal denaturation, a shift from low to high Rth was observed and the temperature at which the shift occurred was higher for the complementary homoduplex dsDNA (black curve) than for both types of heteroduplex dsDNA with mismatches (orange and green curves), as shown in figure 2. The Rth of a naked NCD sample (red curve), an NCD sample functionalized with COOH groups (purple curve), and an NCD sample with ssDNA (blue curve) was also measured for comparison. The reason for this behaviour arises because heteroduplex dsDNA melts at a lower temperature than the full-complementary homoduplex dsDNA due to the intrinsic instability a mismatch will cause in a duplex, as mentioned previously. This strongly signifies the potential of Rth as a DNA-sensor.

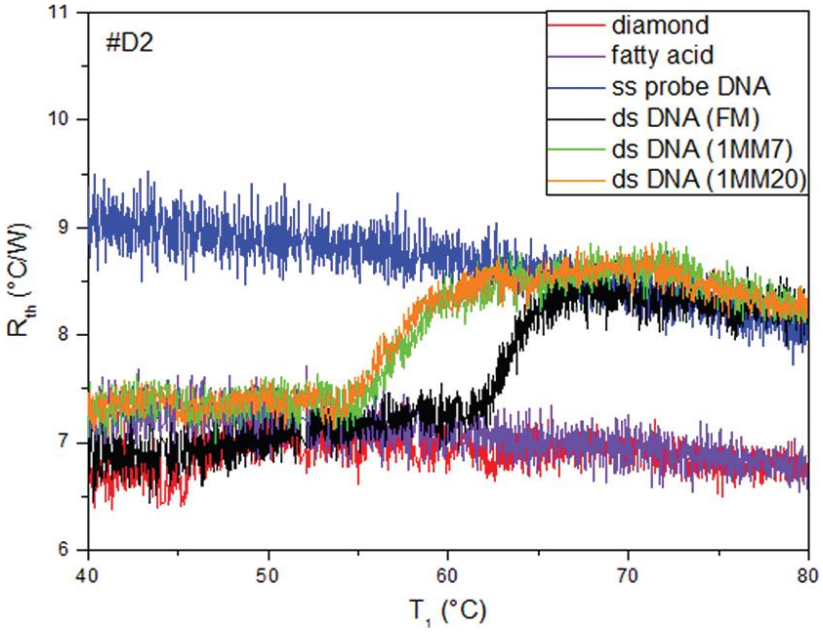

Figure 2. The effect of increasing temperature on the Rth shift of different types of dsDNA duplexes. The signal produced by naked diamond, diamond with fatty acid, and diamond with dsDNA are distinguishable from that of diamond functionalized with ssDNA, indicating the change of DNA conformation during the thermal denaturation. FM: fully matched homoduplex dsDNA, 1MM7: heteroduplex dsDNA with a point mutation at the 7th base, 1MM20: heteroduplex dsDNA with a point mutation at the 20th base.

Although the authors have proved the technique to be viable for mutation detection, it has only been proved to work well with short DNA duplexes. However, in order for this technique to be translated into a fast, label-free and simplified sensor to be used in routine genetic analysis, several aspects need to be optimized.

First, the technique must be compatible with longer strands of DNA, more specifically, to the size of exon fragments. When exons are employed as probes on the sensor, an entire gene can be screened with only a few spots instead of 10,000 spots as in microarrays. Hence, it must become possible to successfully attach longer strands of probe DNA and still detect mutations in these longer fragments using Rth. In this thesis, the consequences of longer strands on the sensitivity of the Rth will be studied using the exons of the PAH gene.

A second aspect to ensure the suitability of Rth in clinical applications is the ability to distinguish homozygotes from heterozygotes.

Materials and Methods

1. Determination of the optimal length of probe DNA strands that can be employed for Rth measurements.

1.1. Immobilization of probe ssDNA

Boron (B)-doped NCD was prepared by chemical vapour deposition (CVD), hydrogenated and functionalized with 10-undecenoic fatty acid via photochemical attachment as shown in figure 3. Synthetic ssDNA strands of lengths varying from 80 to 160 bases, based on exon 6 of the gene for PAH, with an NH_2 group at their 5' end followed by seven adenine bases, were purchased from Integrated DNA Technologies (IDT, Leuven, Belgium) (table 1). This probe DNA was attached to the B-doped-NCD via EDC coupling, as shown in figure 4 [14].

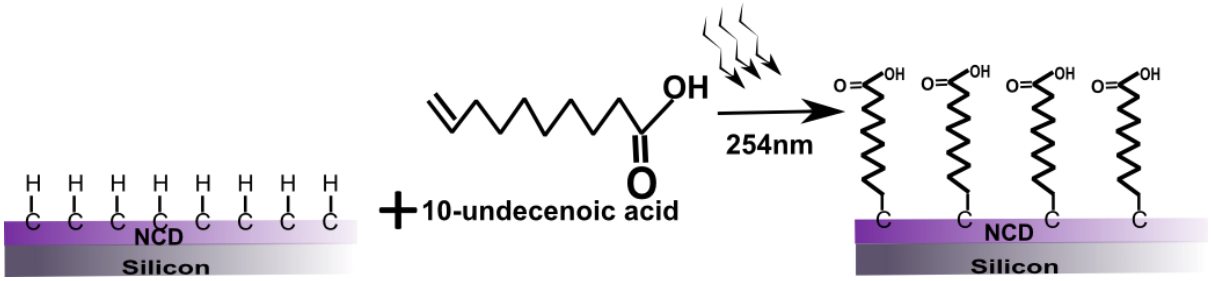

Figure 3. Photochemical attachment of 10-undecenoic acid to hydrogenated NCD.

Table 1. Synthetically produced ssDNA strands of varying length, used as probes for the covalent attachment to B-doped NCD

Length (bases)	Probe ssDNA sequences based on exon 6 of the PAH gene (5'→3')
80	NH_2-AAAAAAATGGGCAGCCCATCCCTCGAGTGGAATACATGGAGGAAGAAAAGAAAACATGGGGCACAGTGTTCAAGACTCTGAAGTCCT
120	NH_2-AAAAAAATGGGCAGCCCATCCCTCGAGTGGAATACATGGAGGAAGAAAAGAAAACATGGGGCACAGTGTTCAAGACTCTGAAGTCCTTGTATAAAACCCATGCTTGCTATGAGTACAATCACATTTT
160	NH_2-AAAAAAATGGGCAGCCCATCCCTCGAGTGGAATACATGGAGGAAGAAAAGAAAACATGGGGCACAGTGTTCAAGACTCTGAAGTCCTTGTATAAAACCCATGCTTGCTATGAGTACAATCACATTTTTCCACTTCTTGAAAAGTACTGTGGCTTCCATGAAGATAAC
197	NH_2-AAAAAAATGGGCAGCCCATCCCTCGAGTGGAATACATGGAGGAAGAAAAGAAAACATGGGGCACAGTGTTCAAGACTCTGAAGTCCTTGTATAAAACCCATGCTTGCTATGAGTACAATCACATTTTTCCACTTCTTGAAAAGTACTGTGGCTTCCATGAAGATAACATTCCCCAGCTGGAAGACGTTTCTCAATTCCTGCAGA

The fatty acid-functionalized NCD was pre-incubated with 30 µl of the NH_2-modified probe ssDNA (300 pmol) for 30 minutes at room temperature. The pre-incubated solution was then removed from the

NCD and mixed with 20 µl of EDC (50 mg/ml) dissolved in 25 mM MES, pH 6, for 2 hours at 4°C. The unbound ssDNA was washed away by incubating the NCD twice in 1X PBS for 5 minutes at room temperature. Then the NCD was incubated in 2X SSC containing 0.5% SDS for 30 minutes at room temperature, again rinsed with 1X PBS at room temperature and stored in fresh 1X PBS at 4°C until hybridization.

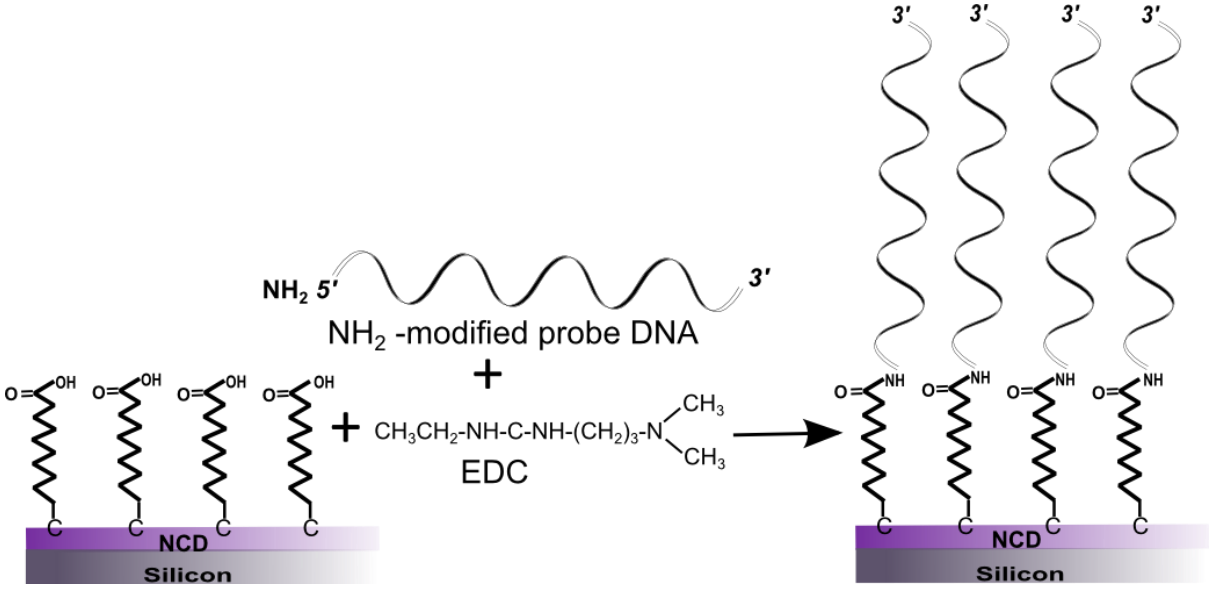

Figure 4. Attachment of NH_2-modified probe DNA to 10-undeconoic acid-functionalized NCD via an EDC reaction.

1.2. Evaluation of the functionality of the attached probe ssDNA

To check if the immobilized probe ssDNA is efficiently attached to the NCD while still remaining available for hybridization, a fluorescently labelled detection probe was designed and purchased from IDT. The detection probe was 30 bases long with an Alexa Fluor® 488 label at its 5' end, and it was designed in such a way that it binds to all the probe ssDNA molecules of different lengths that were immobilized. The sequence of the probe is shown in table 2.

Table 2. Sequence of the detection probe ssDNA.

	Sequence (5'→3')
Detection Probe DNA	Alexa Fluor® 488-CTGTGCCCCATGTTTTCTTTTCTTCCTCCA

For the hybridization, the ssDNA-functionalized NCD was placed in a petridish, and 20 µl of hybridization solution, containing 6 µl of detection probe (100 pmol) and 14 µl of 10X PCR buffer was added to it. This was incubated for 2 hours in an oven at 49°C. In order to prevent evaporation of the hybridization solution, a few drops of water were placed at the edges of the petridish before closing of the lid.

To remove the aspecifically hybridized strands, the functionalized NCD was washed several times. First, the NCD was incubated in 2X SSC containing 0.5% SDS for 30 minutes at room temperature, followed by an incubation in 0.2X SSC for 5 minutes at 44 °C, 5 °C below the hybridization temperature. Then, the NCD was again incubated in 0.2X SSC for 5 minutes, but now at room temperature. Finally, the NCD was rinsed with 1X PBS and stored in 1X PBS at 4°C until the fluorescent measurements.

To confirm whether the probe DNA has been immobilized onto the diamond substrates, a detection probe with Alexa Fluor® 488 was hybridized as mentioned above and the samples were analysed with a Zeiss LSM 510 META Axiovert 200M laser confocal fluorescence microscope. The NCD sample surface was excited with a 488 nm argon-ion laser. Having the pinhole size at 150 µm and the laser intensity at 10% of the maximum of 1.00 ± 0.05 mW, the image was collected at a distance of 5.6 mm through a 10X/0.3 Plan Neofluar air objective with a pixel dwell time of 51.2 µs (~900×900 µm). The detector gain was varied between 800 and 1200 arbitrary units (AU).

To demonstrate that the fluorescence is due to hybridization of the detection probe but not to the NCD substrate itself, photobleaching was performed by illuminating a small region of the NCD surface with 100% laser intensity for 3 minutes.

The fluorescence intensity data were obtained with the help of the AIM4.2 software. In addition to the samples with probe DNA hybridized with detection probe, two NCD samples, one with no EDC during the covalent probe attachment and one with no detection probe DNA, were also analysed. The intensity of the NCD samples was calculated by subtracting the intensity of the NCD which involved no detection probe from the intensity of the ssDNA-functionalized NCD hybridized with detection probe.

2. PKU mutation analysis in the exons of the gene for PAH

2.1 Functionalization of NCD with 3 exons of the PAH gene

Synthetic ssDNA strands reflecting 3 exons of the PAH gene, and spanning the same length range as evaluated in paragraphs 1.1 and 1.2, were purchased from IDT (table 3). The attachment procedure was identical to that described in paragraph 1.1.

Table 3. Synthetically produced ssDNA probes corresponding to 3 exons of the PAH gene, each with a fully complementary or wildtype, and with a prevalently mutated hybridization counterpart, used for Rth studies.

	Length (bases)	Sequence (5'→3')
Exon 5-Probe	105	NH_2AAAAAAAGGCAGACTTACTGGCGGTAGTTGTAGGCAATGTCAGCAAA CTGCTTCCGTCTTGCACGGTACACAGGATCTTTAAAACCCTAGGAGAAAA GAGACACC
Exon 5-Target (wildtype)	98	GGTGTCTCTTTTCTCCTAGGGTTTTAAAGATCCTGTGTACCGTGCAAGACG GAAGCAGTTTGCTGACATTGCCTACAACTACCGCCAGTA AGTCTGCC
Exon 5-Target (mutant) c.473G>A (R158Q)	98	GGTGTCTCTTTTCTCCTAGGGTTTTAAAGATCCTGTGTACCGTGC AAGACAGAAGCAGTTTGCTGACATTGCCTACAACTACCGCCAGTA AGTCTGCC
Exon 9-Probe	73	NH_2-AAAAAAAGGACTTACTGTGGCGAGCTTTTCAATGTATTCATC AGGTGCACCCAGAGAGGCAAGGCCAATTTCC
Exon 9-Target (wildtype)	66	GGAAATTGGCCTTGCCTCTCTGGGTGCACCTGATGAATACATTGA AAAGCTCGCCACAGTAAGTCC
Exon 9-Target (mutant) c.932T>C (p.L311P)	66	GGAAATTGGCCTTGCCTCTCCGGGTGCACCTGATGAATACATTGA AAAGCTCGCCACAGTAAGTCC
Exon 12-Probe	130	NH_2-AAAAAAACTTACTGTTAATGGAATCAGCCAAAATCTTAAGCT GCTGGGTATTGTCCAAGACCTCAATCCTTTGGGTGTATGGGTCGT AGCGAACTGAGAAGGGCCGAGGTATTGTGGCAGCAAAGTTCCT
Exon 12-Target (wildtype)	123	AGGAACTTTGCTGCCACAATACCTCGGCCCTTCTCAGTTCGCTAC GACCCATACACCCAAAGGATTGAGGTCTTGGACAATACCCAGCAG CTTAAGATTTTGGCTGATTCCATTAACAGTAAG

Exon 12-Target (mutant) c.1222C>T (R408W)	123	AGGAACTTTGCTGCCACAATACCTTGGCCCTTCTCAGTTCGCTAC GACCCATACACCCAAAGGATTGAGGTCTTGGACAATACCCAGCAG CTTAAGATTTTGGCTGATTCCATTAACAGTAAG

2.2 Hybridization with synthetically produced fully complementary (wildtype) and mutated target ssDNA

For the hybridization, two types of target ssDNA were used for each exon probe: a fully complementary, or wildtype, ssDNA target, and a ssDNA target that differed from the wildtype at one location, reflecting a very prevalent PKU-associated mutation in the Belgian population (table 3). These ssDNA targets were also purchased from IDT. As explained in paragraph 1.2, the ssDNA-functionalized NCD was placed in a petridish, and 40 µl of hybridization solution, containing 12 µl of target ssDNA (100 pmol) and 28 µl of 10X PCR buffer, was added to it. This was incubated for 2 hours in an oven at 55°C. In order to prevent evaporation of the hybridization solution, a few drops of water were placed at the edges of the petridish before closing of the lid.

To remove the aspecifically hybridized strands, the functionalized NCD was washed several times. First, the NCD was incubated in 2X SSC containing 0.5% SDS for 30 minutes at room temperature, followed by an incubation in 0.2X SSC for 5 minutes at 50°C, 5°C below the hybridization temperature. Then, the NCD was again incubated in 0.2X SSC for 5 minutes, but now at room temperature. Finally, the NCD was rinsed with 1X PBS and stored in 1X PBS at 4°C until Rth measurements.

2.3. Rth measurements

The sensor cell, displayed in figure 6, consists of a copper block, to the back of which a heating element is attached, and in the front of the copper block the functionalized NCD substrate is stuck with the help of conducting silver paint. Heat is regulated by applying a potential of 0 V to 10 V to the copper block, which has a resistance (R) of 22.2 Ω, with the help of which the power (P) is determined as explained below. A sensing area is created on the NCD with the help of an O-ring made of rubber allowing the DNA to be in contact with the aqueous environment at any time during the measurement. The temperature T1 of the copper block and the temperature T2 of the liquid inside the flow cell are monitored with the help of a thermocouple.

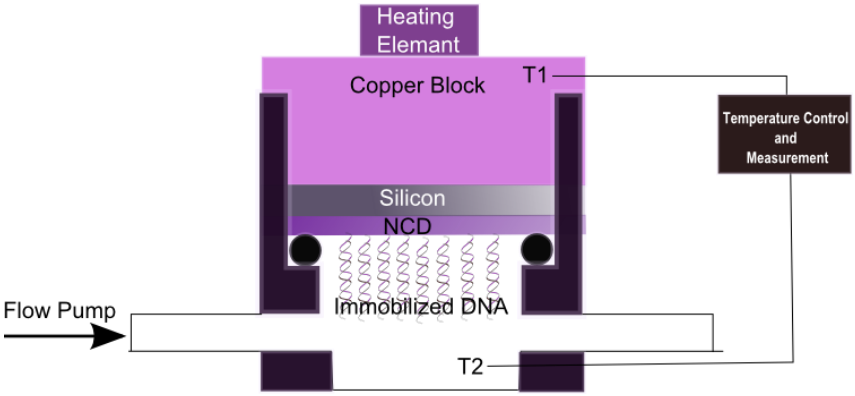

Figure 5. Schematic representation of the Rth sensor cell and its components.

NCD samples, functionalized with either homoduplex or heteroduplex exon 5, 7, 9, or 12 dsDNA, all synthetically produced, were mounted in the above described setup. The temperature T1 of the copper block was raised from 35°C to 85°C, to assure thermal denaturation of the dsDNA, and cooled back to 35°C at a rate of 1°C/minute. The heat transfer resistance (Rth) was calculated by dividing ΔT (T1-T2)

by the power (P) of the system needed to control the temperature, as shown in equation 1. The power can be determined by dividing the square of the applied voltage (V) by the resistance (R) of the device, which is 22.2 Ω, as shown in equation 2.

$$\text{Equation 1: } Rth = \frac{T1-T2}{P}$$

$$\text{Equation 2: } P = \frac{V^2}{R} = \frac{V^2}{22.2\Omega}$$

2.4 Preparation of target ssDNA from real samples

To translate the Rth measurements performed on synthetically produced homo- and heteroduplexes to an application suitable for the use of patient material, PCR reactions needed to be optimized to generate the exons of the PAH genes of patients, for hybridization with the attached exon probes on the NCD.

2.4.1. Primer design

The first step in order to achieve this, is to design 14 pairs of primers (table 6) to specifically amplify all of the 12 exons of the PAH gene, to yield amplicons of maximally 150 bp in length, using the NCBI primer-BLAST tool. Exon 3 and 6 were divided into two fragments as they were longer than the persistence length of dsDNA, which is 150 bp, predicted to be the limit of Rth. The primers were analyzed and evaluated in OligoAnalyzer 3.1, based on the criteria shown in table 4, so that they will not form any secondary hairpin loops, self-dimers, or heterodimers.

Table 4. Primer design evaluation criteria.

Primer length	**17-28 bases**
G/C content	**40-60%**
Melting temperature	**55-65°C**
Maximum number of G/C runs	**3-4**
Maximum accepted stability of hairpins (ΔG)	**>-3 kcal/mol**
Maximum accepted stability of self or cross dimers (ΔG)	**>-6 kcal/mol**
Maximum accepted stability of heterodimers (ΔG)	**>-6 kcal/mol**

2.4.2 Extraction of DNA from whole blood

Genomic DNA was extracted from blood of a healthy donor by the phenol-chloroform and ethanol precipitation method. Red blood cells (RBC) were first eliminated using 1X hemolysis buffer. The rest of the WBC were treated with cell lysis buffer to disrupt and release all their cell components. First, the proteins were degraded using the enzyme Proteinase K, and separated from the nucleic acids by phenol-chloroform. Then, the nucleic acids were recovered by precipitation in 70% ethanol, followed by drying. The DNA was finally resuspended in 100 µl of milli-Q water and stored at -20°C.

2.4.3. Optimization of PCR

2.4.3.1 Determination of the optimal annealing temperature

The best annealing temperature of the primers was determined by performing a gradient PCR for all of the primer pairs. All the reactions were carried out in a My Cycler™ Thermal Cycler (Bio-Rad, Nazareth, Belgium). The PCR reaction mix of 20 µl contained 1X PCR buffer with 1.5 mM Mg^{2+}, 0.5 pmol of forward primer/reverse primer, 4 pmol of dNTPs, 1 unit of *Taq* DNA polymerase, 200 ng of genomic DNA and milli-Q water. The reaction mix was thermally cycled as follows: 95°C for 5 minutes, 35 cycles of 95°C for 2 seconds, 45-61°C for 10 seconds, 72°C for 30 seconds, and one cycle of 72°C for 6 minutes.

2.4.3.2 Determination of optimal Mg^{2+} concentration

For those exons that had a low yield of PCR products, the concentration of Mg^{2+} was optimized. The thermal conditions and reaction mixture were the same as in the gradient PCR described in paragraph 2.4.3.1, except the Mg^{2+} concentration was increased from 1.5 mM to 4 mM.

All the PCR products were analyzed in a 3% agarose gel and the length was compared with a 25 bp DNA ladder from Invitrogen™. For concentration analysis, SmartLadder (Eurogenetic) was loaded along the samples and the concentrations were analyzed on a Bio-Rad gel documentation system with the aid of Quantity One® version 4.6.3 software.

In addition to the agarose gel electrophoresis, the concentration and the purity of the DNA was also checked on a NanoDrop 2000 UV-Vis Spectrometer.

2.4.4. Generation of ssDNA from dsDNA PCR products

In order to allow hybridization of healthy donor DNA to the exon-functionalized NCD, the PCR products of the exons of PAH need to be made single-stranded. Two techniques were compared to reach this goal: linear amplification and Lambda Exonuclease digestion.

2.4.4.1. Linear amplification

The PAH exons were first amplified by PCR under optimized conditions obtained by gradient PCR and Mg^{2+} optimization, described in paragraph 2.4.3.1and 2.4.3.2Purification of the resulting exon amplicons was done with Exo-SAP-IT to remove the unused primers and dNTPs. In brief, 2 µl of Exo-SAP-IT was added to 10 ng/µl of PCR product, followed by incubation at 37°C for 15 minutes for the activation of the enzyme, and at 80°C for 15 minutes to inactivate the enzyme.

The purified products were used as starting material in linear amplification. In linear amplification, only one of the two primers is added to the PCR mix, to ensure amplification of only one of the two strands and the generation of single-stranded amplicons. The reaction mix of 20 µl contained 1X PCR buffer with 1.5 mM Mg^{2+}, 0.5 pmol of FITC-labelled forward primer, 4 pmol of dNTPs, 1 unit of *Taq* DNA polymerase, 50 ng of purified PCR products, optimized Mg^{2+} concentration and milli-Q water. The FITC label is necessary to allow the analysis with Genescan® Analysis software of the ABI Prism® 310 Genetic Analyzer. The annealing temperature and cycle number of the linear amplification were optimized as follows: 95°C for 5 minutes, 20/25/30 cycles of 95°C for 2 seconds, optimized hybridization temperature for 10 seconds, 72°C for 30 seconds and one cycle of 72°C for 6 minutes.

The linearly amplified products were further purified through a Sephadex™ G-50 column at 3200 RPM for 2 minutes.

The purified products were analyzed in Genescan® Analysis mode of the ABI PRISM® 310 Genetic Analyzer. For analysis, 0.25 µl of purified products were combined with 24.25 µl of Hi-Di™ Formamide to make them single-stranded, and 0.5 µl of GS-400 HD ROX SIZE STD as a length ladder. The solution was incubated at 95°C for 5 minutes and immediately put on ice for 1 minute to avoid formation of any secondary structures.

2.4.4.2. Lambda Exonuclease digestion

The PAH exons were first amplified by PCR, in a reaction mix of 20 µl, containing 1X PCR buffer with 1.5 mM Mg^{2+}, 0.5 pmol forward primer, 0.5 pmol of phosphorylated reverse primer, 4 pmol of dNTPs, 1 unit of *Taq* DNA polymerase, 200 ng of genomic DNA and milli-Q water. Phosphorylation is necessary, since only the strands with a 5' phosphorylation are substrates for the 3'→5' exonuclease activity of Lambda Exonuclease. The reaction mix was thermally cycled as follows: 95°C for 5 minutes, 35 cycles of 95°C for 2 seconds, optimized hybridization temperature for 10 seconds, 72°C for 30 seconds, and 72°C for 6 minutes and one cycle of 72°C for 6 minutes.

Purification of the resulting phosphorylated PCR products was done with Exo-SAP-IT to remove the unused primers and dNTPs. In brief, 2 µl of Exo-SAP-IT was added to 50 ng of PCR product, followed by incubation at 37°C for 15 minutes for the activation of the enzyme, and at 80°C for 15 minutes to inactivate the enzyme. The remaining salts and FITC labels were removed by spinning the DNA through a Sephadex G-50 column at 3200 RPM for 2 minutes.

To remove the phosphorylated strands, the purified and phosphorylated dsDNA was then treated with Lambda Exonuclease by incubating 10 µl of solution, containing 5 units of Lambda Exonuclease, 1X Lambda Exonuclease Reaction Buffer and 0.1-2 µg of dsDNA, for 30 minutes at 37°C, to activate the enzyme, and 30 minutes at 70°C, to deactivate the enzyme.

Finally, the remaining monophosphates and other salts were removed by spinning through a Sephadex™ G-50 column at 3200 RPM for 2 minutes.

2.5 Hybridization with wildtype target ssDNA from healthy donors

Hybridization of the wildtype target ssDNA was not done in solid phase, as described in paragraph 2.2, but in solution. The reason for using 1200 pmol of target DNA for hybridizing with the 300 pmol of attached probe ssDNA is to increase the hybridization efficiency by adding an excess of target ssDNA. However, hybridization in solid phase is not as efficient as hybridization in solution. So in this case, the hybridization of target to probe was done in solution and then covalently bound in doublestranded form to NCD, as shown in figure 6. This served to reduce the amount of target DNA needed, and hence to reduce cost of target DNA generation.

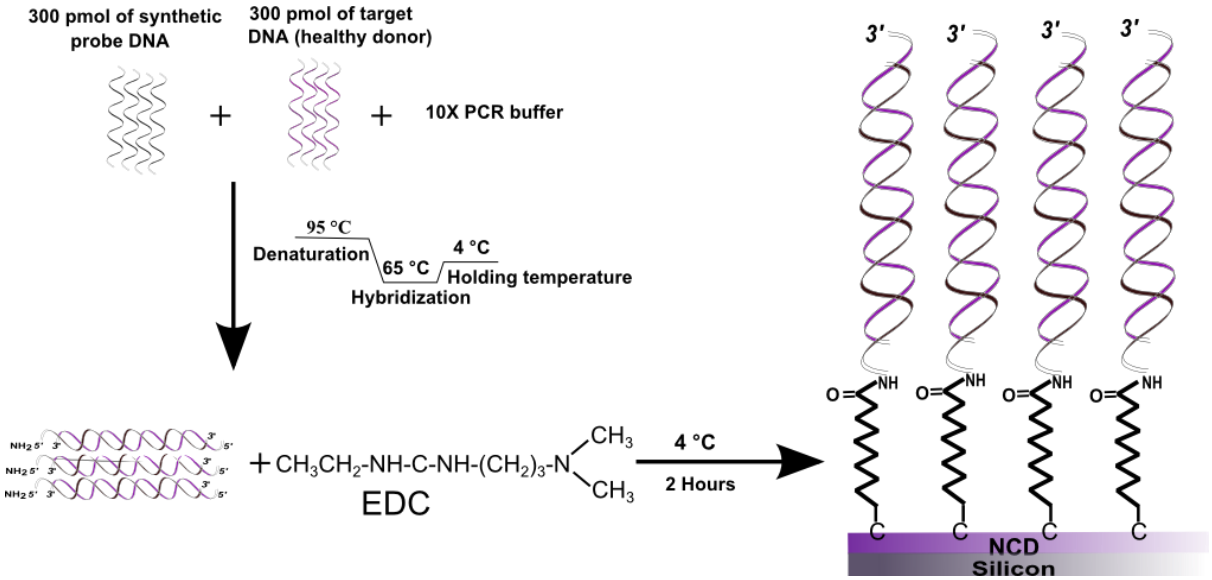

Figure 6. Functionalization of NCD with dsDNA after hybridizing the target ssDNA to the probe ssDNA in solution.

In this method, 3 µl of 100 pmol of synthetic probe ssDNA and 3 µl of 100 pmol of target ssDNA generated from healthy donors was mixed with 14 µl of 10X PCR buffer and thermally cycled as follows: 95°C for 5 minutes, 65°C for 45 minutes, 4°C for 1 minute. Then, 20 µl of 1 mg/ml EDC in 25 mM MES buffer, pH 6, was added to the reaction mixture and was used for functionalization as described in paragraph 1.1. The other washing steps were carried out exactly as mentioned in paragraph 2.2.

2.6. Rth measurements with healthy donor material

A homoduplex was immobilized on NCD as described in paragraph 2.5. The measurements were done as described above in paragraph 2.3.

3. Surface plasmon resonance (SPR)

SPR was also studied for its suitability to detect SNPs. All the experiments were performed in a BiacoreTM T200 (GE Healthcare, Diegem, Belgium) system at 25°C with a streptavidin (SA)-modified sensor chip. Biotinylated probe ssDNA (table 5), purchased from IDT, was injected at a flow rate of 10 µl/min aiming to achieve 1000 response units (RU). Once the expected range was reached, 1X PCR buffer was injected at a flow rate of 10 µl/min with a contact time of 2 minutes, to wash away the aspecifically bound strands. This step was repeated for five times. Target ssDNA that was fully complementary or contained a mutation with respect to the probe, also purchased from IDT, was then injected at the same flow rate, and with a contact time of 8 minutes. In order to remove the unhybridized strands, another washing step with 1X PCR buffer at the same flow rate and with a contact time of 2 minutes was performed.

After the successful hybridization of both types of target ssDNA, denaturation studies were performed with different concentrations of NaOH starting from 1 mM to 20 mM. The flow rates and contact times were optimized during the study. All the results were analysed from real-time sensorgrams generated by the BIAevaluation 2.1 software.

Table 5. Synthetically produced biotinylated probe ssDNA probe based on the PAH gene, with a fully complementary or wildtype, and with a mutated hybridization counterpart, employed for SPR studies.

	Sequence (5'→3')
Probe	Biotin-AAAAAAACCCCTGCAGCCCATGTATACCCCCGAACC
Target (wildtype)	GGTTCGGGGGTATACATGGGCTGCAGGGG
Target (mutant)	GGTTCGGGGGTATACATGGGCTCCAGGGG

Results and Discussions

4. Determination of optimal length of probe DNA strands that can be employed for Rth measurements

The confocal microscopic images (panel A) and the intensity profile of the NCD (panel B) functionalized as mentioned in paragraphs 1.1 and 1.2 is shown in figure 7. The NCD sample that was treated with ssDNA without EDC and the sample where no detection probe DNA was hybridized, clearly show that the fluorescence intensity was much lower than the samples where the ssDNA was covalently attached and allowed to hybridize with detection probe. In these negative samples, the intensity was solely due to the background. The green spots are unremoved accumulations of detection probe DNA. The reason for the accumulation might be because of the small length of the detection probe, which causes it to get trapped within the layer of probe ssDNA. The graph shown in panel B of figure 7 depicts the intensity profile of the samples that were functionalized with probe ssDNA of different lengths. The intensity decreases with increasing length of the probe ssDNA.

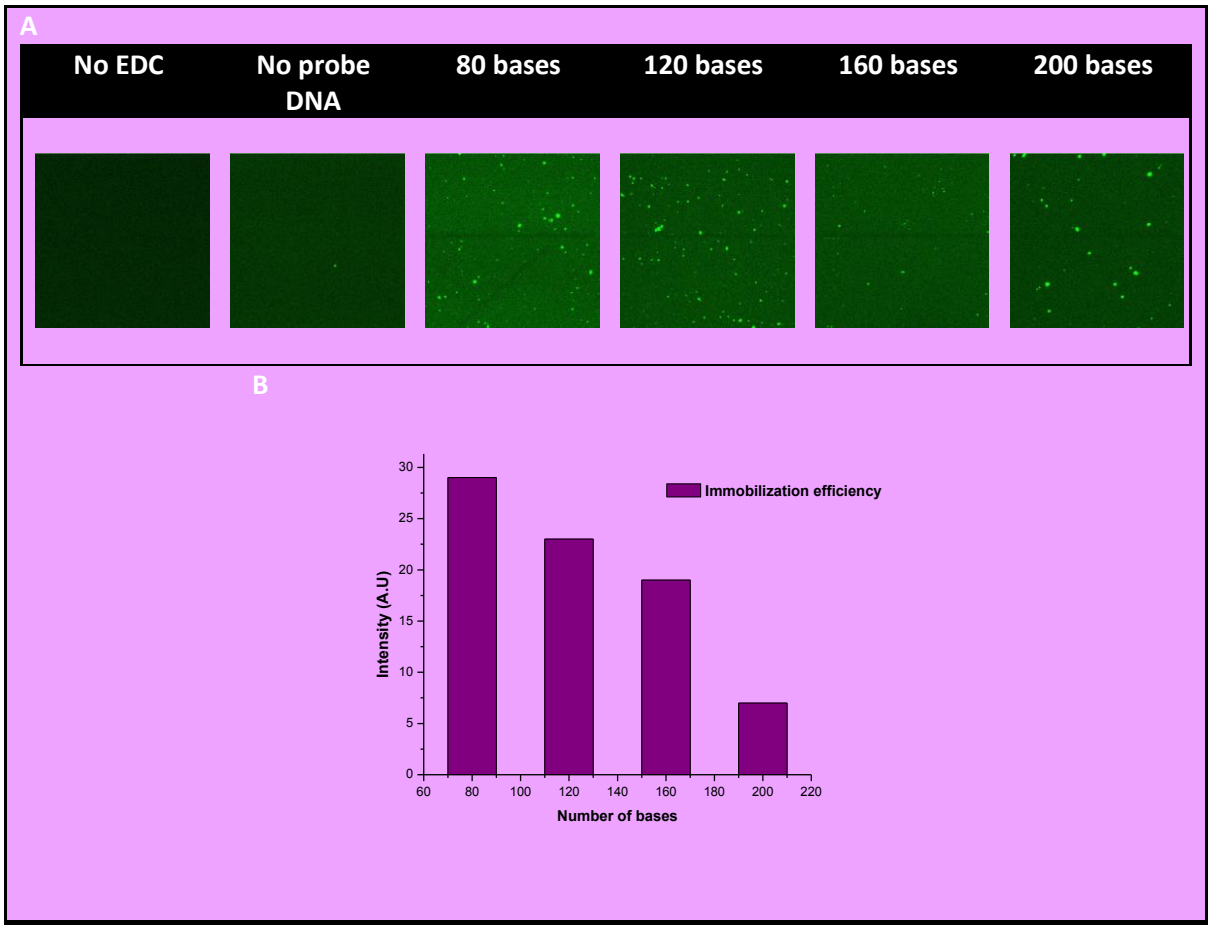

Figure 7. Confocal microscopic images (A) and the intensity profile of functionalized NCD (B) after the covalent attachment of synthetic ssDNA of different lengths and the hybridization with an Alexa Fluor® 488-labeled detection probe.

The photobleaching line confirms that the fluorescence is due to the attached ssDNA, not due to the NCD substrate itself. The longer the ssDNA molecules to be attached, the more space they will take up on the NCD since they will not remain upright but form a meshwork on the surface, and the less ssDNA will fit per cm^2. However, the NCD functionalized with ssDNA of 200 bases is still clearly distinguishable from the negative controls.

The conclusion that can be drawn from this experiment is that probe ssDNA with a length of up to 200 bases can still be immobilized successfully, although the highest efficiencies are reached with lengths until 160 bases. This means that all exons of the gene for PAH could be efficiently attached.

5. PKU mutation analysis in the exons of the gene for PAH

NCD samples were functionalized with synthetic strands with the sequence of exon 9, 5, 12 and 7 and hybridized to synthetically produced wildtype or mutated target ssDNA containing prevalent SNPs (table 3) as mentioned in paragraphs 2.1 and 2.2. Rth measurements were carried out during the thermal denaturation of the formed homo- and heteroduplexes, as mentioned in paragraph 2.3. After the measurements, Rth and P were calculated according to equations 1 and 2, respectively. Rth was then plotted as a function of T1, as shown in figure 8.

Figure 8 shows the change in the Rth during the thermal denaturation of exon 9, which is 66 bp long. The black line represents the behaviour of the heteroduplex, formed through the hybridization of the covalently attached probe to the target ssDNA containing the SNP c.932T>C (p.L311P), and the red line represents the homoduplex sequence formed through the hybridization between probe and wildtype target ssDNA. Heteroduplex and homoduplex showed Rth shifts at 59°C and 71°C, respectively. The lower temperature at which the heteroduplex melts from doublestranded to singlestranded reflects its intrinsic instability due to the mismatch that is present. This result is comparable to the results obtained by Van Grinsven *et al.*, where they used shorter 29-mer sequences, and it proves that longer strands can also be employed for Rth measurements.

Similar measurements were made with hetero- and homoduplexes of exon 5, 12, and 7, which are 98 bp, 123 bp and 150 bp in length, respectively. All the measurements had a similar pattern of Rth behaviour as compared to figure 8, as shown in figure 9, 10, and 11. In figure 9, showing the results for exon 5, the noise level was higher because the measurement was done before the PID controller setting was improved. The measurements for exon 7, 9, and 12 were made after the improvement, which reduced the noise by a factor of 3. The refinements of the flow cell are discussed elsewhere [ref]. The temperatures where the Rth shifts from the doublestranded to the singlestranded level, reflecting the melting temperatures of the different exons, can be found in table 5.

From the measurements it is clear that diagnosing PKU-associated SNPs in longer strands of up to 123 bp is possible with Rth. Strands that spanned 150 bp or more had Rth shift for both homo- and heteroduplex but they were random and indescribable. However, it should be noted that the found melting temperatures vary when different NCD samples are used that were produced in different batches.

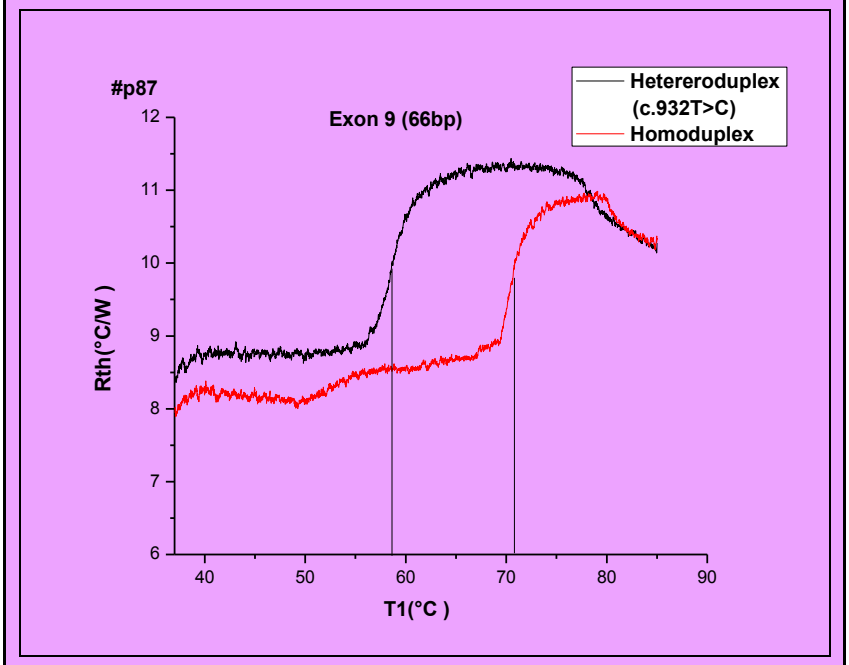

Figure 8. Rth as a function of T1 during the thermal denaturation of homoduplex and heteroduplex exon 9 of 66 bp.

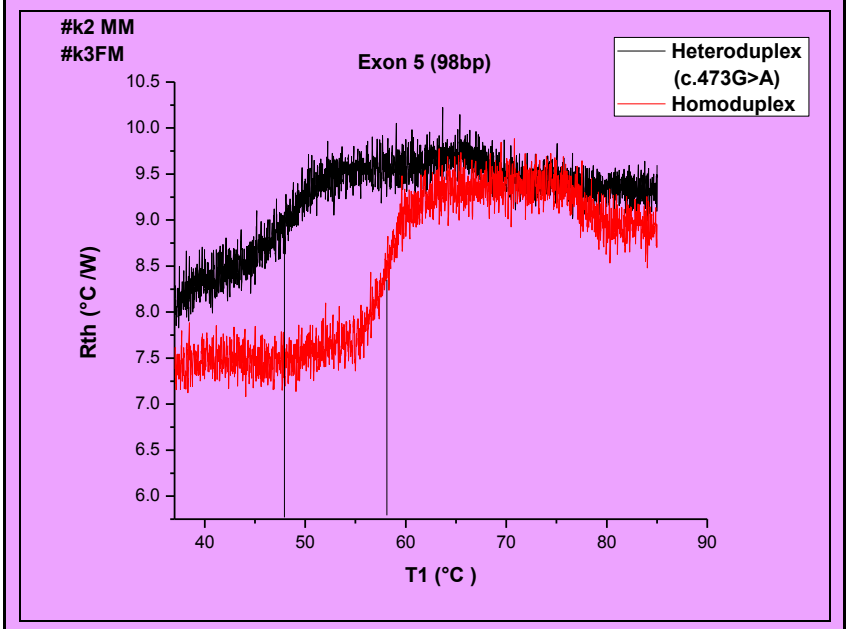

Figure 9. Rth as a function of T1 during the thermal denaturation of exon 5 of 98 bp.

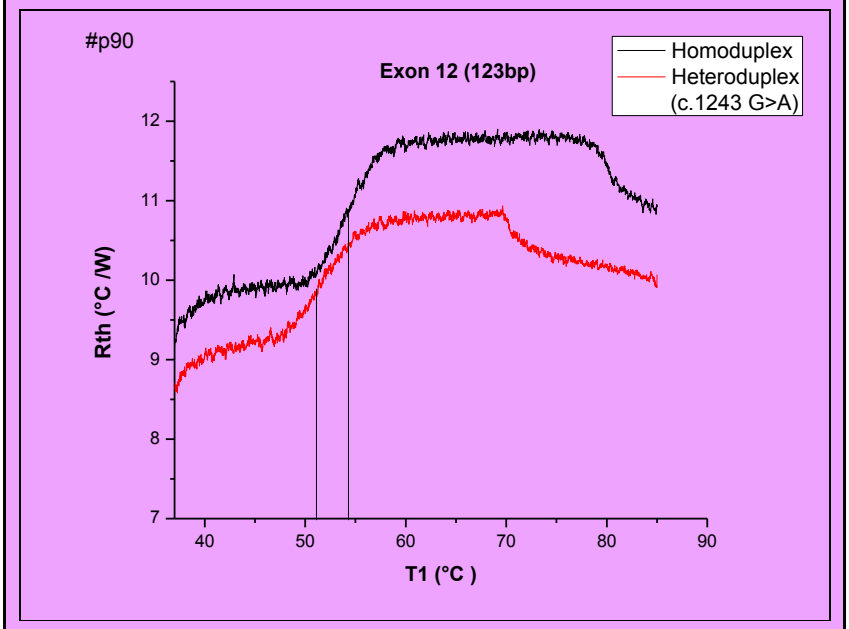

Figure 10. Rth as a function of T1 during the thermal denaturation of exon 12 of 123 bp.

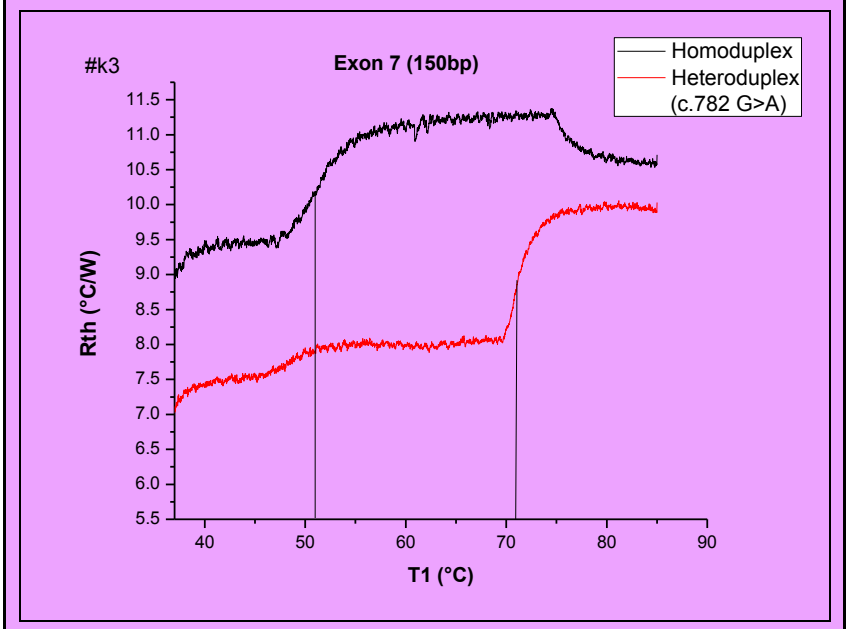

Figure 11. Rth as a function of T1 during the thermal denaturation of exon 7of 150 bp.

Table 5. Melting temperatures of homoduplex and heteroduplex DNA, as deduced from their Rth graphs in figure 8-11.

	Length (bp)	Homoduplex	Heteroduplex
Exon 9	66	71 °C	59 °C
Exon 5	98	59 °C	49 °C
Exon 12	123	54 °C	51 °C
Exon 7	150	51 °C	71 °C

The reason for this variation might be associated with the varying thickness and roughness of the NCD samples from different growth batches. Also, the method employed for hybridizing with mutated target DNA could vary due to human handling and the lower efficiency of heteroduplex formation. Therefore, a standardized method should be developed to bring consistent and reproducible results. However, despite the variations in the absolute melting temperatures when different NCD samples were used, the homoduplexes always melted at a higher temperature than the heteroduplexes. This at least highlights the suitability of Rth measurements for mutation detection relative to a wildtype, homoduplex reference.

6. Preparation of target ssDNA from clinical patient samples

6.1 Primer design

In order to translate this method into a technique suitable for clinical use, the wildtype exon probes on the NCD need to be hybridized to target exons coming from PKU patients and healthy controls. From the results obtained with synthetic strands, it was concluded that the maximum length of DNA strands that can be used for mutation detection with Rth was 150 bp. Having this as a basis, the exons of the PAH gene were analysed, and, besides exon 7, exon 3 was above this length. For this reason, exon 3 and 6 were divided into two overlapping sequences. Primer pairs to amplify all exons of PAH were specifically designed as mentioned in paragraph 2.4.1 (table 6).

Table 6. Primer pairs designed to amplify the 12 exons of the PAH gene, with their respective melting temperatures and GC content.

Primer Name	Sequence (5'→3')	Length (bases)	GC content (%)	Melting temperature (°C)
1 Forward	AGCCAGAGACCTCACTCCCG	20	66	65
1 Reverse	GTGGCTCACCTGTCCAAAGT	20	63.9	55
2 Forward	TCTTATCCTGTAGGAAACAAGC	22	59.9	40.9
2 Reverse	ACTGACCTCAAATAAGCGCA	20	61.5	45
3.1 Forward	TTCTCTCTTCTAGGAGAATGATGT	24	60.4	37.5
3.1 Reverse	AGGCAGGCTACGTTTATCCA	20	62.8	50
3.2 Forward	TGCCTGCTCTGACAAACATC	20	62.2	50
3.2 Reverse	CCTCTAATTCTTACCTGTGTCTTTC	25	60.6	40
4 Forward	TGTGTTTCAGTGCCCTGGTT	20	64.1	50
4 Reverse	GCATCCAGTTCCGCTCCATA	20	63.6	55
5 Froward	GGTGTCTCTTTTCTCCTAGGGT	22	62.5	50
5 Reverse	GGCAGACTTACTGGCGGTAG	20	63.5	60
6.1 Forward	GAGACACCTATTTTGTGCCTGTA	23	62	43.5
6.1 Reverse	CAAGGACTTCAGAGTCTTGAACA	23	61.8	43.5
6.2 Forward	ACCCATGCTTGCTATGAGTACA	22	63.3	45.5

6.2 Reverse	GGACTTACTCTGCAGGAATTGAGA	24	63.4	45.8
7 Forward	ATCCCAGCTTGCACTGGTTT	20	64.3	50
7 Reverse	TACTCACGGTTCGGGGGTAT	20	64	55
8 Forward	GCTTTCTGTCTTTCAGTGACATC	23	61.9	43.4
8 Reverse	CACAGACCTATAACTAGAAGGCTAA	25	61.4	40
9 Forward	GGAAATTGGCCTTGCCTCTCT	21	64.3	52.4
9 Reverse	GGACTTACTGTGGCGAGCTT	20	63.3	55
10 Forward	CCATTCCAGATTTACTGGTTTACTG	25	61.3	40
10 Reverse	TACCTGTAATTCACCAAAGGATGAC	25	62.3	40
11 Forward	GGGCCTACAGTACTGCTTATCA	22	62.9	50
11 Reverse	ACCTTACTTTCTCCTTGGCATCA	23	63.5	43
12 Forward	AGGAACTTTGCTGCCACAATA	21	62.2	42.8
12 Reverse	CTTACTGTTAATGGAATCAGCCAAA	25	61.5	36

6.2 Determination of optimal annealing temperature and Mg^{2+} concentration

Table 7. Summary of the optimized annealing temperatures, as determined through gradient PCR, and Mg2+ concentrations for each primer pair

Exon	Template concentration (ng)	Magnesium concentration (mM)	Annealing temperature (°C)	Length (bp)	Concentration (ng/µl)
1	200	1.5	65	99	20.43708
2	100	3	51	127	14.56809
3.1	100	2	51	112	16.3048
3.2	200	1.5	51	104	24.40177
4	200	1.5	51	89	13.97331
5	200	1.5	51	98	20.62932
6.1	200	1.5	51	111	29.19456
6.2	200	1.5	51	117	20.8347
7	200	1.5	51	150	11.47094
8	200	1.5	51	127	12.91084
9	200	1.5	51	66	7.731814
10	200	1.5	51	108	15.48026
11	200	1.5	51	146	18.41872
12	200	1.5	51	123	11.2074

A gradient PCR was performed with each primer pair, to find the optimal annealing temperatures, as mentioned in paragraph 2.4.3.1. The template DNA amount for most of the exons was 200 ng. Except for exon 2 and 3.1 is was 100 ng. The annealing temperature of exon 1 was chosen to be 65°C as there was aspecific amplification at lower annealing temperatures. All other primer pairs gave a good yield with annealing temperatures of 51°C. After this gradient PCR, the exons that still gave a rather low yield as compared to the others were improved by increasing the concentration of Mg^{2+}. The Mg^{2+} concentration was limited to 1.5 mM for all the exons except for exon 2 and 3.1. Figure 12 shows the results of the PCR reactions for each primer pair performed with the optimized conditions in a 3% agarose gel. Each exon fragment is well represented with acceptable yield.

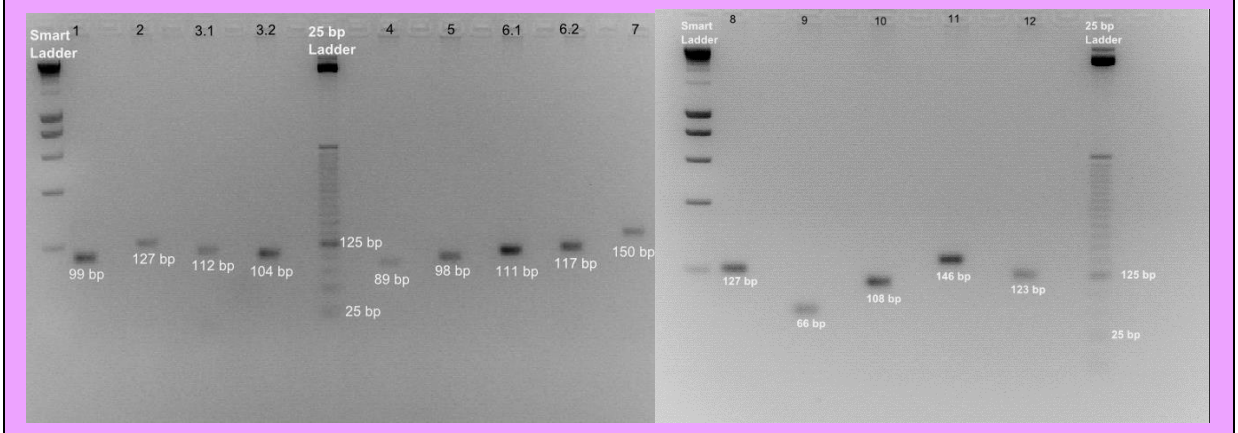

Figure 12. Resulting agarose gel after using each primer pair in PCR reactions under optimized conditions, as summarized in table 9, to obtain all exon fragments of the PAH gene.

6.3 Generation of ssDNA from dsDNA PCR products

In order to be suitable for hybridization to the exon probes attached to NCD, the generated patient and healthy control exons in paragraph 6.2 need to be made singlestranded. Two methods were explored for generating ssDNA from healthy controls: linear amplification and Lambda Exonuclease digestion.

6.3.1. Linear amplification

Linear amplification was performed as mentioned in paragraph 2.4.4.1. After amplifying the exons under optimized conditions with normal primers (table 7 and figure 12), linear amplification was performed by employing a FITC-labelled forward primer. Originally, the goal of the FITC label was to allow evaluation of the size of the product using the ABI PRISM® 310 Genetic Analyzer, and also to give a clear idea about the hybridization efficiency by evaluation under the confocal microscope. According to the standard optimized protocol, only 50 ng of template could be used as a starting material. This limits the amount of the ssDNA that can be produced during one reaction and increases the amount of the enzyme usage. Even though the length of the strands can be determined in the Genescan® Analysis mode of the ABI PRISM® 310 Genetic Analyzer, it fails to quantify the amount in terms of nanograms. However, linear amplification was optimized under the conditions as shown in table 8.

Table 8. Optimized conditions for linear amplification using a FITC-labelled forward primer.

Exon	Number of cycles	Hybridization temperature (°C)	Size (bases)	Height
1	35	65	100.41	6194
2	20	51	129	5671
3.1	25	51	113.44	4589
3.2	25	51	104	1048
4	25	51	90.81	6479
5	20	51	98	2155
6.1	30	51	112	6614
6.2	30	51	119	5958
7	30	51	151.48	3064

8	30	51	129.98	2131
9	20	51	67	3132
10	20	51	109.88	6538
11	30	51	146.83	4744
12	20	51	123.95	6382

In the ABI PRISM® 310 Genetic Analyzer, the ssDNA of different, unknown size, labelled with FITC is separated according to its length together with a size marker containing ssDNA fragments of known lengths, and labelled with another fluorophore. The sizes of the unknowns are determined optically by the Genescan® analysis mode, using the size marker as a ladder. Figure 13 shows the Genescan® result of exon 6.1. The length of the strands in bases is represented on the X-axis and the Y-axis represents the peak height (no units), indicating yield. A peak was observed at expected the length of 112 b. However, there were several smaller peaks close to the length of 20 b that reflect unused primers and primer dimers. It is obvious that huge amount of primers are not being used during the amplification. In another case, besides showing a peak close to the expected length of 99 b (100.41 b), the Genescan® result of exon 1 had several peaks between the lengths of primers and primer dimers and the length of the actual product (99 b), as is shown in figure 14, indicating that there was aspecific amplification. The Genescan® results of other exons can be found in the supplemental information.

Although the intended ssDNA product of the desired length was produced during linear amplification, it was challenging to determine the concentration of the FITC-labelled target ssDNA. In addition, using FITC-labelled primers did not yield as much product as when using the normal unlabelled primer. Efforts were made to determine the concentration of the generated ssDNA fragments in the microarray mode of the NanoDrop 2000 UV-Vis Spectrometer, but it was difficult to discriminate the concentration of the linearly amplified product from the aspecifically amplified products and the primers and primer dimers. Hence, a bulk concentration was obtained with contributions from all of these. For this reason, this method was not further used in generating target ssDNA, and it needs further optimization for bulk production and application in hybridization assays.

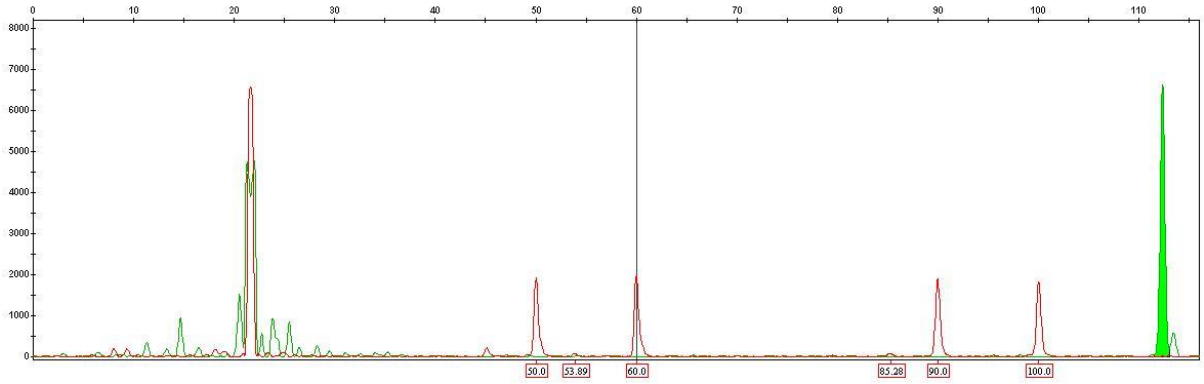

Figure 13. Genescan® result of singlestranded exon 6.1, produced through linear amplification. The size marker is shown as red peaks, while the FITC-labeled products produced during linear amplification are shown as green peaks.

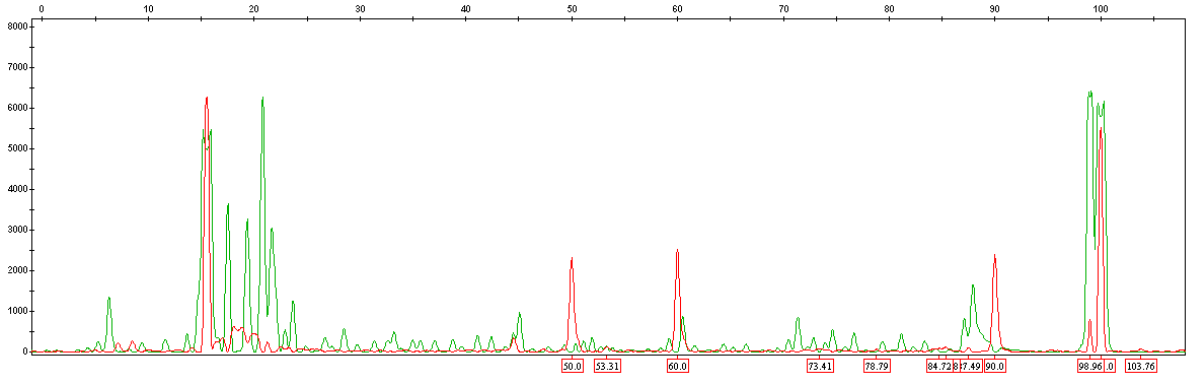

Figure 14. Genescan® result of singlestranded exon 1, produced through linear amplification. The size marker is shown as red peaks, while the FITC-labeled products produced during linear amplification are shown as green peaks.

6.3.2. Lambda Exonuclease digestion

In this method dsDNA amplicons were prepared with a phosphorylated reverse strand and then converted to ssDNA with the help of the enzyme Lambda Exonuclease, as mentioned in paragraph 2.4. 4.2. The concern with the previous method was the purity of the eventual ssDNA product. In addition to the product of interest, also many aspecific or partially amplified ssDNA fragments were formed. Lambda Exonuclease digestion on the other hand, produced pure products. This became obvious when amplicons with a FITC-labelled forward strand and a phosphorylated reverse strand were treated with Lambda Exonuclease and analysed in Genescan®, as shown in figure 15).

The first peak which is found at 20 b corresponds to unused primer, which is negligible as the peak is very tiny. Two additional peaks are visible at 98 b and 99 b, and they both represent exon. The variation in the length by one base is because of the presence of an additional adenine base, which occurs sometimes as *Taq* DNA polymerase naturally has the ability of non-template addition of adenine [20]. This was also occasionally observed during linear amplification which can be found supplemental information. However, both peaks are not high, as the exons were initially amplified under conditions optimized for unlabelled primers.

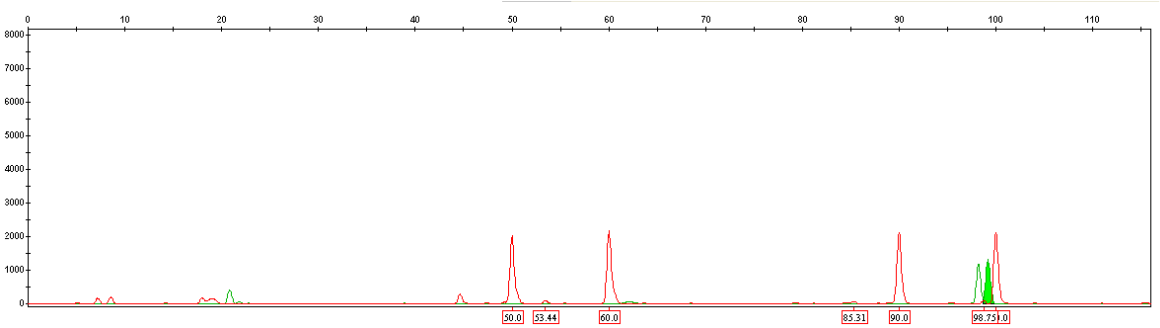

Figure 15. Genescan® result of singlestranded exon 5, produced through Lambda Exonuclease digestion. The size marker is shown as red peaks, while the FITC-labeled products produced during PCR are shown as green peaks.

A.

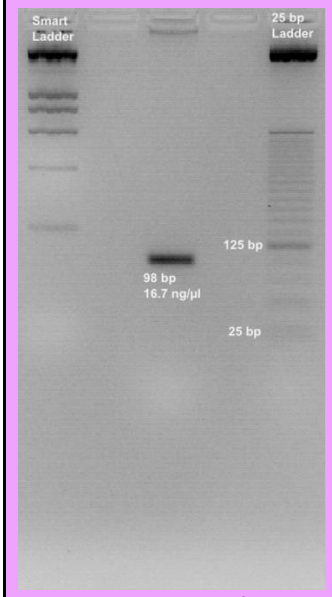

Agarose gel, 3%, of exon 5 after Lambda Exonuclease digestion and purification

Batch 1

	Concentration (ng/µl)	Volume (µl)
Concentrated	208.8	42
After treating with Lambda Exonuclease	128.2	50
After sephadex column purification	98.6	40

= 121.9 pmol in total volume

B.

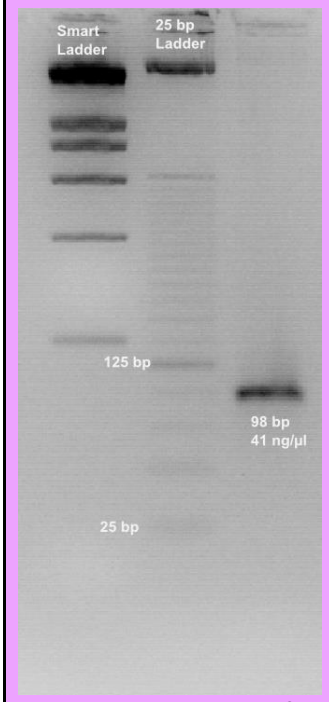

Electrophoretogram of the final product after lambda exonuclease treatment and sephadex column purification. The band accounts for 33% of undigested dsDNA.

Batch-2

	Concentration (ng/µl)	Volume (µl)
Concentrated	274.6	42
After treating with Lambda Exonuclease	173.1	60
After sephadex column purification	121.3	55

= 206.27 pmol in total volume

Figure 16. Production of 300 pmol of exon 5 ssDNA from dsDNA through Lambda Exonuclease digestion in two batches. A) Batch 1 yielded 121.9 pmol, and B) batch 2 yielded 206.27 pmol.

Since this method yielded pure exon target ssDNA, it was chosen to provide the ssDNA for further measurments. Approximately 300 pmol of exon 5 target ssDNA was generated using this method as shown in figure 16. This amount was the absolute minimum that was required, since 300 pmol of probe ssDNA was used to attach to NCD with the EDC reaction. The 300 pmol was produced in two batches, and the concentrations at every stage of the procedure were determined with the NanoDrop 2000 UV-Vis Spectrometer. To check if all of the dsDNA from the original PCR was converted into ssDNA, the final product was loaded onto a 3% agarose gel, which only shows dsDNA. A band of 98 bp was still observed, of about 41 ng/µl. This indicates that the digestion to ssDNA was not complete, and that 33% of the DNA still remains in doublestranded form. However, this was not a big concern as the strands will be denatured before hybridizing to the attached probe DNA and only the complementary strands will hybridize with the probe.

Since Lambda Exonuclease digestion still involves the use of the expensive enzymes Lambda Exonuclease, Exonuclease I, and Shrimp Alkaline Phosphatase, the latter two as part of the Exo-SAP-IT kit, a new, less expensive, method for preparing patient material is still required.

7. Rth measurements with real samples

Exon 5 target ssDNA from healthy donors was generated through Lambda Exonuclease digestion as mentioned above in paragraph 6.3.2. Since the cost for producing ssDNA through Lambda Exonuclease digestion was fairly expensive, an adapted protocol for hybridization and NCD functionalization was developed. The generated target ssDNA of exon 5 was hybridized in solution to probe exon 5 in a 1:1 ratio, equalling 300 pmol of total DNA, as described in paragraph 2.5, and covalently bound to NCD as described in paragraph 1.1. Rth measurements were made as mentioned in paragraph 2.3. There was a steep increase of Rth as shown in figure 17. The dsDNA started melting at 66°C and was transformed completely into ssDNA at 82°C. Unlike synthetic strands, the Rth level of ssDNA of donor material was high and it had an irregular shift, showing a biphasal increase. The reason for this behaviour is not clear, since only one type of duplex is attached to the NCD. It could be because of the *Taq* DNA polymerase which introduces errors at a rate of 10^{-4} to 10^{-5} per nucleotide. Hence, the target ssDNA could contain mismatches compared to the wildtype probe, causing a mixture of heteroduplexes and homoduplexes to be attached to the NCD. However, this biphasal behaviour is not visible after hybridizing a synthetic mixture of SNP-containing and wildtype target ssDNA to previously attached probe ssDNA, or after attaching 2 types of homoduplex dsDNA differing significantly in melting temperature (data not shown).

However, this thesis confirms the possibility of transforming the previously described Rth device (van Grinsven *et al.*, 2012), capable of distinguishing short homoduplexes from heteroduplexes into a device suitable for diagnosing SNPs in real clinical samples.

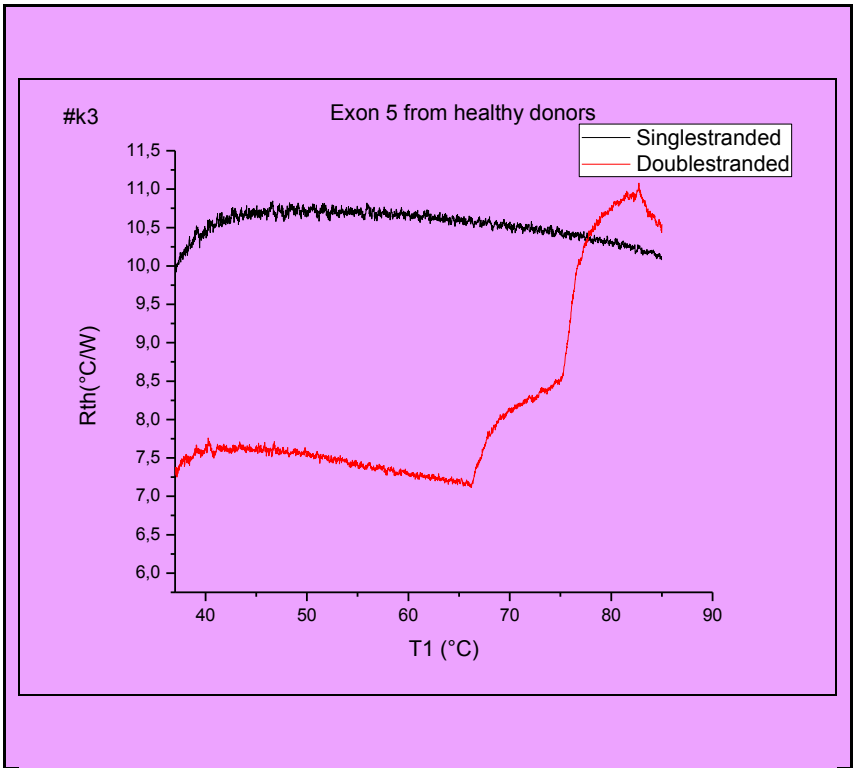

Figure 17. Rth as a function of T1 during the thermal denaturation of exon 5 generated from a healthy donor.

8. Surface Plasmon Resonance

To evaluate if other, well-established, technologies could be employed for something other than their primary application field, SPR was used to study mutation analysis. The biotin-labelled probe DNA was immobilized onto SA-functionalized SPR chips as mentioned in paragraph 3 until the response level reached about 1000 R.U. For the continuation of the experiment, shown in figure 18, this level was reset to zero. Either fully complementary target ssDNA or target ssDNA containing a SNP was injected to form either homoduplexes or heteroduplexes on the chip surface, respectively. In order to remove aspecifically hybridized sequences, 1X PCR buffer was injected as mentioned in paragraph 3. After this, the response level increased to 385 R.U. due to the hybridization of the complementary target DNA. During the formation of the heteroduplexes, the level increased comparably, to 396 R.U. Denaturation was performed, and it was found to be most effective when 5 mM NaOH was used at a flow rate of 1µl/minute with a contact time of 5 minutes. After denaturation of the homoduplex, the response level decreased to 201 R.U. After denaturation of the heteroduplex, the level decreased to 183 R.U. This experiment was repeated three times to evaluate reproducibility.

The hybrid stability index [ref] was calculated using the following formula, given in equation 3, to determine the level of dissociation.

$$Equation\ 3: Hybrid\ stability\ index = \frac{R.U.final - R.U.residual}{R.U.final - R.U.initial}$$

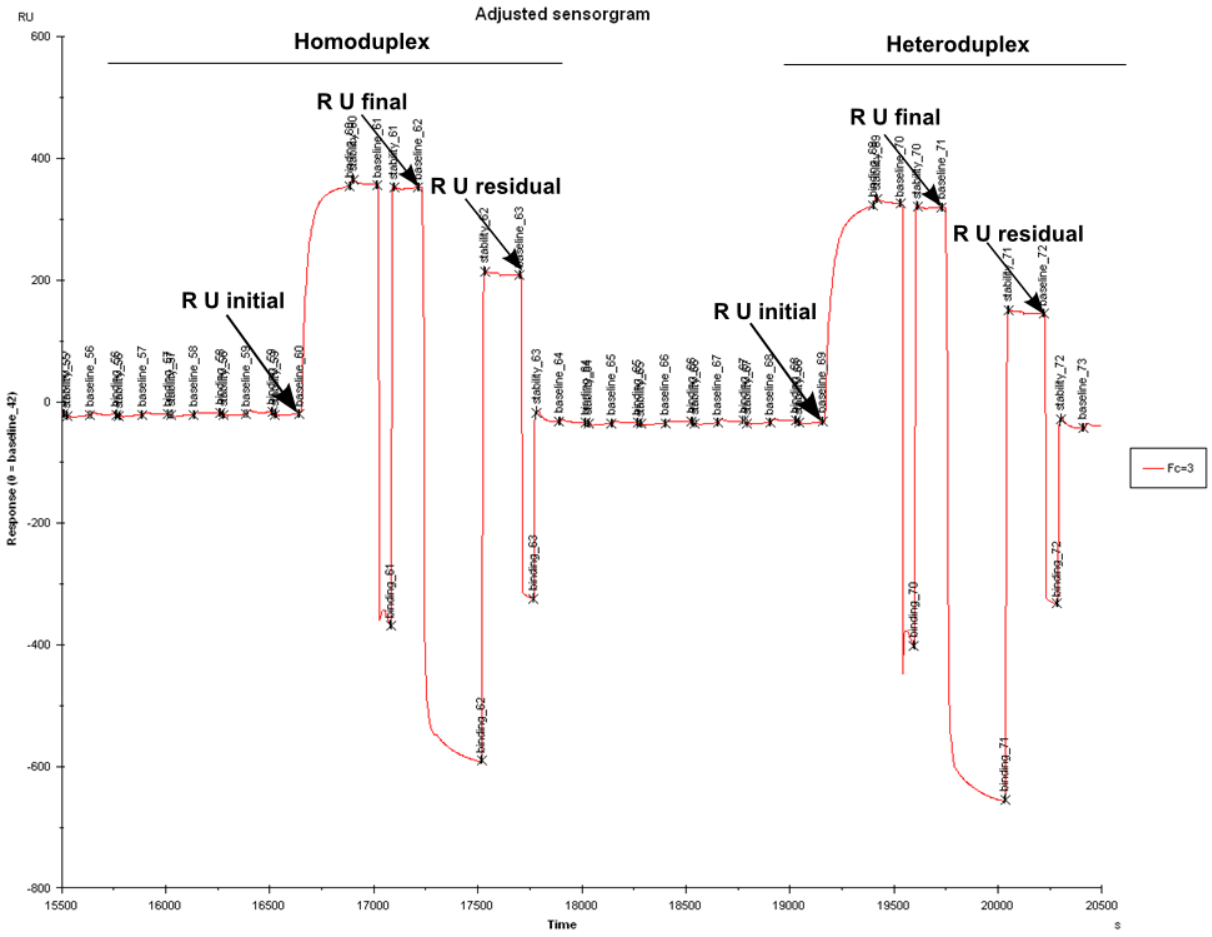

Figure 18. SPR sensorgram during formation and denaturation of homo- and heteroduplexes of 29 bp based on the PAH gene.

It gives an indication of the ratio between the amount of hybridized duplexes and the amount of denatured singlestrands left. R.U. initial is the response level before hybridization, R.U.final is the response level after hybridization, and R.U.residual is the response level after denaturation (figure 18). The results of both types of duplexes are given in table 9.

Table 9. Hybrid stability index calculations of 29 bp homo- and heteroduplex DNA.

Trial		R.U.final – R.U.initial	R.U.final – R.U.residual	Hybrid stability index
1	Homoduplex	396.2	182.9	0.46
	Heteroduplex	384.9	201.7	0.52
2	Homoduplex	371.9	144.3	0.38
	Heteroduplex	353.0	175.4	0.49
3	Homoduplex	363.8	110.1	0.30
	Heteroduplex	343.8	126.0	0.36

The level of dissociation of homo- and heteroduplexes confirms that the fully complementary homoduplex is more stable than the heteroduplex, nicely confirming the results described by Giordana, et al,. 1999 [21].SPR is a well-established technique used for studying the interaction of biomolecules, especially receptor-ligand interaction. It has not been used widely for studying DNA hybridization and

denaturation, only few have reported on diagnosing SNP using SPR. In this study we have demonstrated the possibility of real-time detection of SNPs in a 29-mer sequence via SPR. This method is label free and simple, but requires expensive instrumentation. Further research with longer strands of homo- and heteroduplex are necessary to transform this technique to be used for diagnosing SNP in real clinical situations.

Summary and Conclusion

This thesis was started form where van Grinsven *et al.*, 2012 proved the Rth as a technique for diagnosing SNPs in short DNA fragments. The overall objective was to transform the device to be suitable to diagnose mutations in real clinical situations. The first prerequisite was to evaluate the technique with exon-size DNA, which would simplify an eventual array by allowing to screen an entire gene with only a few spots. In this thesis we have proved the possibility of using the Rth device for diagnosing mutations in the exons of the PAH gene.

As a first step we determined the immobilization efficiency of longer DNA by immobilizing synthetic probe ssDNA of different lengths onto NCD and hybridizing it with a small detection probe that was labelled with Alexa Fluor® 488. Through confocal fluorescence microscopy the immobilization was found to be still effective at 200 b. This indicated that all exons of PAH, being smaller than 200 b, could be functionally bound to NCD.

Following this, the suitability of these long strands for Rth measurements was checked. We designed synthetic strands encompassing the sequence of 4 PAH gene exons 5, 7, 9, and 12 to be used as probes on the NCD, and their fully complementary and SNP-containing hybridization counterparts for homo- and heteroduplex formation. The duplex lengths spanned 98 to 150 bp. Duplexes that were less than 100 bp (exon 5 and 9) showed an Rth shift during thermal denaturation and it was easy to discriminate between homo- and heteroduplex. Duplexes that were more than 100 b (exon 12) showed an Rth shift, but it became more difficult to discriminate between homo- and heteroduplex. Duplexes that were around 150 b (exon 7) showed an Rth shift, but the relative denaturation temperatures as determined by Rth were random for homo- and heteroduplex. This suggests that the DNA length limit for Rth measurements is somewhere between 123 and 150 b. A feasible explanation is that the longer dsDNA fragments become, the more they approach the persistence length of dsDNA (150 bp) and tend to curve instead of remain upright. This will disturb the heat transfer through the spaces in between the immobilized dsDNA fragments, resulting in a decreased resolution between ssDNA and dsDNA, shown by a decreased absolute Rth change upon denaturation.

Having determined the optimal length that is suitable for Rth measurements, it became clear that exon 3 and 6 needed to be divided into two overlapping fragments to be immobilized as probes. To generate hybridization material from real donor samples, primers were designed to specifically amplify the 12 exons of the PAH gene that would yield amplicons within the optimal length range. In total, 14 primer pairs were designed (2 sets for exon 3 and 6) and they were optimized to produce acceptable amounts of amplicons.

The next part of the study was to produce ssDNA form these amplicons. Initially, we tried to produce ssDNA by linear amplification. However, the products, although containing the intended target ssDNA, also included aspecifically amplified products. This diluted our intended product. Hence, this method was abandoned for generating target ssDNA.

To overcome the above mentioned problem, Lambda Exonuclease digestion was used to convert the dsDNA into ssDNA. The end product generated by this method yielded pure ssDNA amplicons. So, this method was preferred for generating target ssDNA. However, the cost for producing ssDNA target material through this method was very high as it involved purification with Exo-SAP-IT. Inspite of this, we generated 300 pmol of target ssDNA of PAH exon 5 from a healthy donor through this method.

To compensate for the high production cost of ssDNA through Lambda Exonuclease digestion, we developed a new protocol for the formation and attachment of duplexes to NCD, where the target and

probe ssDNA were hybridized in solution in a 1:1 ratio, before binding the duplex to NCD with EDC. In solution the molecules have more degrees of freedom than when one of them is attached to a solid, making an excess unnecessary. The hybridized homoduplex was subjected to Rth measurements. We observed a shift in Rth and this suggests that this technique can be employed to detect mutations in real samples. However, the observed biphasal Rth increase is not completely understood. The error-proneness of *Taq* polymerase generating a mixture of ssDNA molecules, and thus a mixture of homo- and heteroduplexes on the surface, combined with the variability associated with NCD sample growth, could provide a tentative hypothesis.

Further studies are needed to address some issues. The sensor cell itself is not thermally isolated, and the results varied when different NCD samples were used. The device and diamond growth process must be improved to provide consistent and reproducible results.

Another challenge that we observed during this study was the production of target ssDNA from clinical samples. Cheaper methods, like asymmetric PCR, must be explored for generating sufficient amounts of target ssDNA.

However, the problem of requiring such high amounts of target could also be resolved if the size of the Rth device was reduced to accommodate for less amount of material for measurement. Miniaturization will also reduce noise, increase reproducibility and decrease production cost.

A last point of future attention is to develop a method for discriminating patients with a homozygous and a heterozygous mutation.

References

1. Scriver, C. R. (2007). The PAH gene, phenylketonuria, and a paradigm shift.*Human mutation*, *28*(9), 831-845.
2. Zschocke, J., Haverkamp, T., & Møller, L. B. (2012). Clinical utility gene card for: Phenylketonuria. *European Journal of Human Genetics*, *20*(2).
3. Lodewyckx, L., Vandevyver, C., Vandervorst, C., Van Steenbergen, W., Raus, J., & Michiels, L. (2001). Mutation detection in the alpha-1 antitrypsin gene (PI) using denaturing gradient gel electrophoresis. *Human mutation*, *18*(3), 243-250.
4. Karam, P. E., Al-Hamra, R. S., Nemer, G., & Usta, J. (2012). Spectrum of mutations in Lebanese patients with phenylalanine hydroxylase deficiency.*Gene*.
5. Muyzer, G., & Smalla, K. (1998). Application of denaturing gradient gel electrophoresis (DGGE) and temperature gradient gel electrophoresis (TGGE) in microbial ecology. *Antonie van Leeuwenhoek*, *73*(1), 127-141.
6. Sassolas, A., Leca-Bouvier, B. D., & Blum, L. J. (2008). DNA biosensors and microarrays. *Chemical reviews*, *108*(1), 109.
7. Yao, D., Yu, F., Kim, J., Scholz, J., Nielsen, P. E., Sinner, E. K., & Knoll, W. (2004). Surface plasmon field-enhanced fluorescence spectroscopy in PCR product analysis by peptide nucleic acid probes. *Nucleic acids research*,*32*(22), e177-e177
8. Liebermann, T., & Knoll, W. (2000). Surface-plasmon field-enhanced fluorescence spectroscopy. *Colloids and Surfaces A: Physicochemical and Engineering Aspects*, *171*(1), 115-130.
9. Marrazza, G., Chianella, I., & Mascini, M. (1999). Disposable DNA electrochemical biosensors for environmental monitoring. *Analytica chimica acta*, *387*(3), 297-307.
10. Minunni, M., Tombelli, S., Mariotti, E., Mascini, M., & Mascini, M. (2001). Biosensors as new analytical tool for detection of Genetically Modified Organisms (GMOs). *Fresenius' journal of analytical chemistry*, *369*(7), 589-593.
11. Mascini, M., Palchetti, I., & Marrazza, G. (2001). DNA electrochemical biosensors. *Fresenius' journal of analytical chemistry*, *369*(1), 15-22.
12. Takenaka, S., Yamashita, K., Takagi, M., Uto, Y., & Kondo, H. (2000). DNA sensing on a DNA probe-modified electrode using ferrocenylnaphthalene diimide as the electrochemically active ligand. *Analytical chemistry*, *72*(6), 1334-1341.
13. Jiang, M., & Wang, J. (2001). Recognition and detection of oligonucleotides in the presence of chromosomal DNA based on entrapment within conducting-polymer networks. *Journal of Electroanalytical Chemistry*, *500*(1), 584-589.
14. Gooding, J. J. (2002). Electrochemical DNA hybridization biosensors. *Electroanalysis*, *14*(17), 1149-1156.
15. Arora, K., Prabhakar, N., Chand, S., & Malhotra, B. D. (2007). Ultrasensitive DNA hybridization biosensor based on polyaniline. *Biosensors and Bioelectronics*, *23*(5), 613-620.
16. van Grinsven, B., Vanden Bon, N., Strauven, H., Grieten, L., Murib, M., Jiménez Monroy, K. L., ... & Wagner, P. (2012). Heat-transfer resistance at solid–liquid interfaces: a tool for the detection of single-nucleotide polymorphisms in DNA.*ACS nano*, *6*(3), 2712-2721.
17. Shendure, Jay, and Hanlee Ji. "Next-generation DNA sequencing." *Nature biotechnology* 26, no. 10 (2008): 1135-1145.
18. http://www.illumina.com/Documents/products/Illumina_Sequencing_Introduction.pdf
19. Christiaens, P., Vermeeren, V., Wenmackers, S., Daenen, M., Haenen, K., Nesládek, M., ... & Wagner, P. (2006). EDC-mediated DNA attachment to nanocrystalline CVD diamond films. *Biosensors and Bioelectronics*, *22*(2), 170-177.

20. Magnuson, V. L., Ally, D. S., Nylund, S. J., Karanjawala, Z. E., Rayman, J. B., Knapp, J. I., ... & Collins, F. S. (1996). Substrate nucleotide-determined non-templated addition of adenine by Taq DNA polymerase: implications for PCR-based genotyping and cloning. *BioTechniques*, *21*(4), 700-709.
21. Feriotto, G., Lucci, M., Bianchi, N., Mischiati, C., & Gambari, R. (1999). Detection of the ΔF508 (F508del) mutation of the cystic fibrosis gene by surface plasmon resonance and biosensor technology. *Human mutation*, *13*(5), 390-400.

Supplemental Information

Optimization of Linear amplification

Exon 2

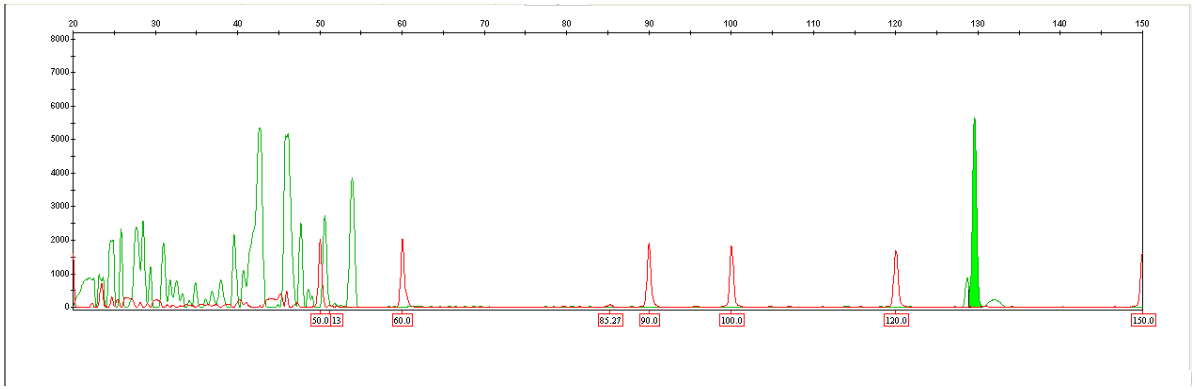

Exon 3.1

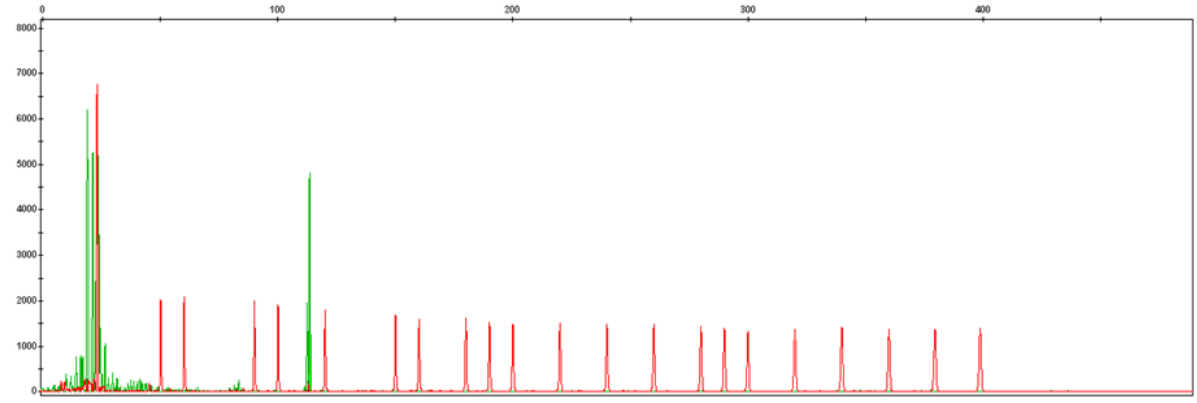

Exon 3.2

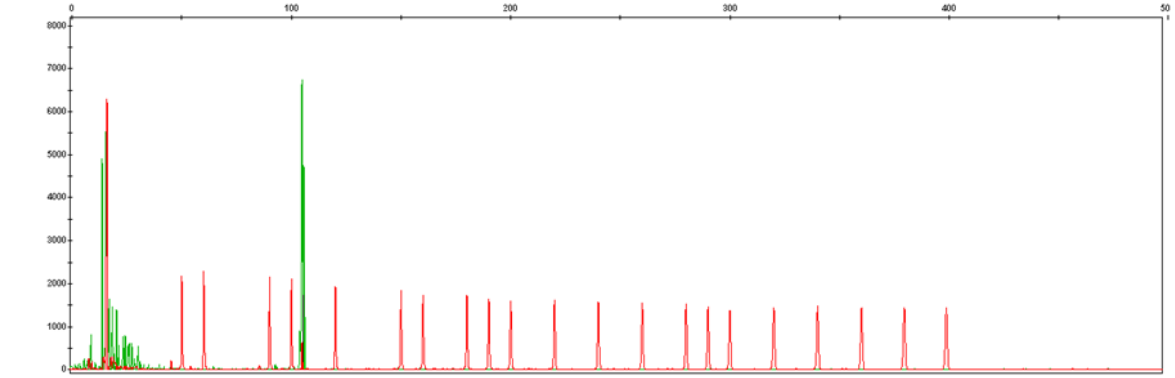

Exon 4

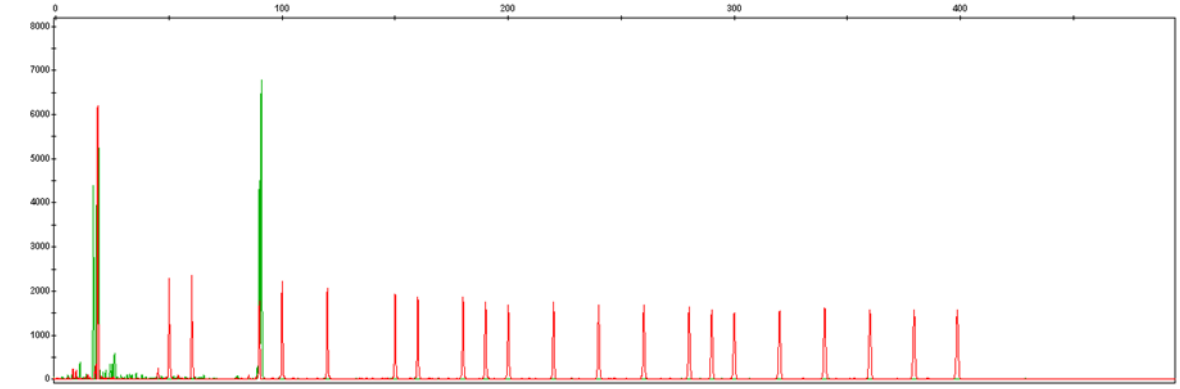

Exon 5

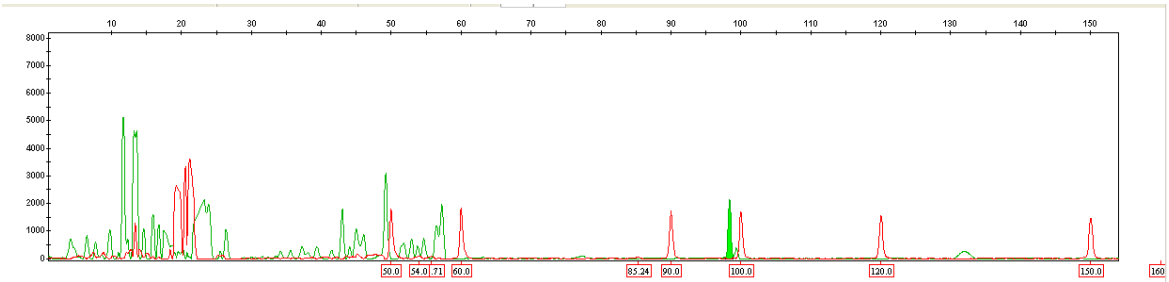

Exon 5

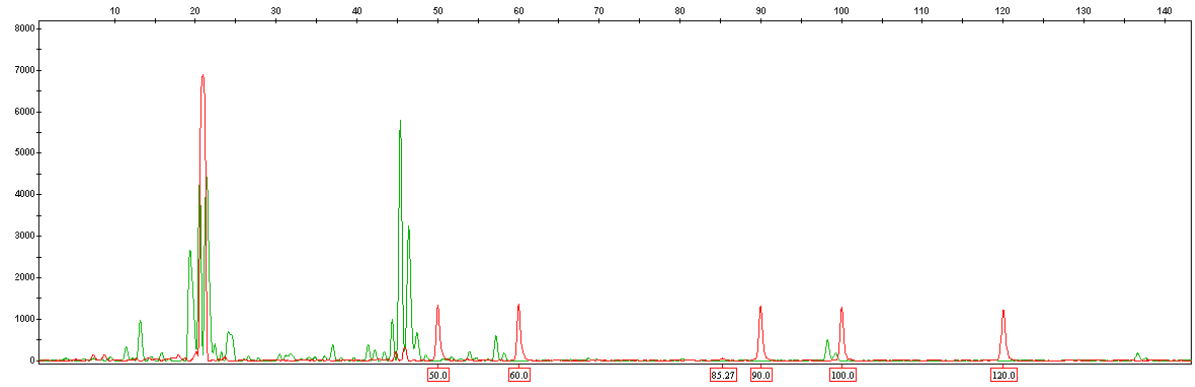

Exon 6.2

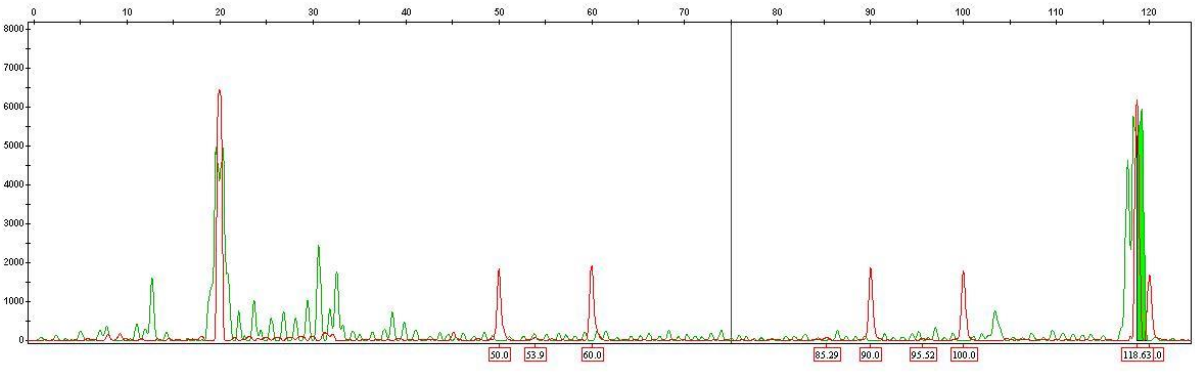

Exon 7

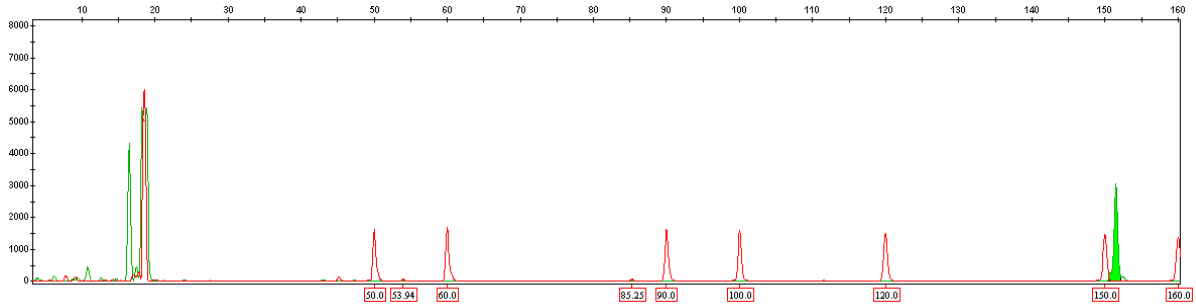

Exon 8

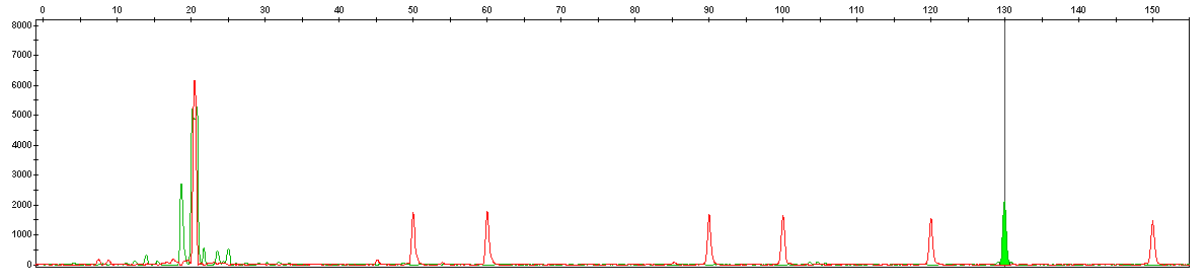

Exon 9

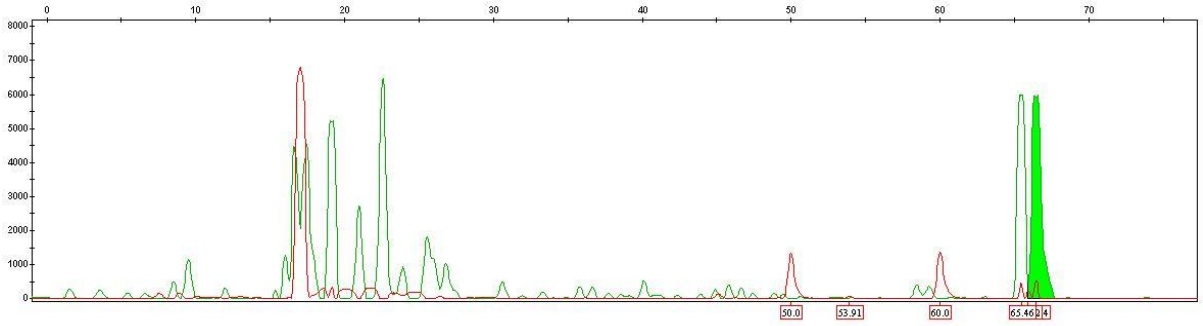

Exon 10

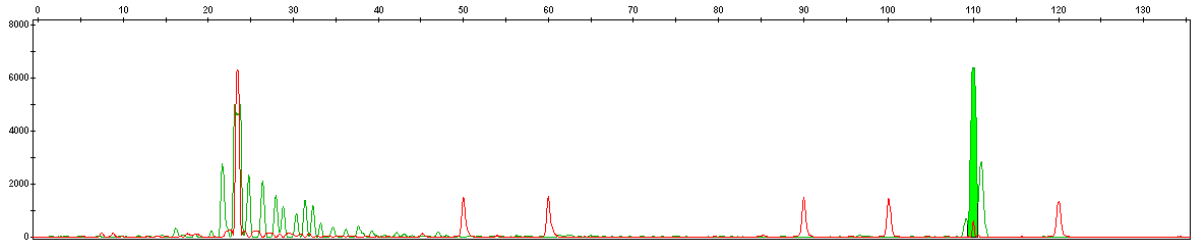

Exon 11

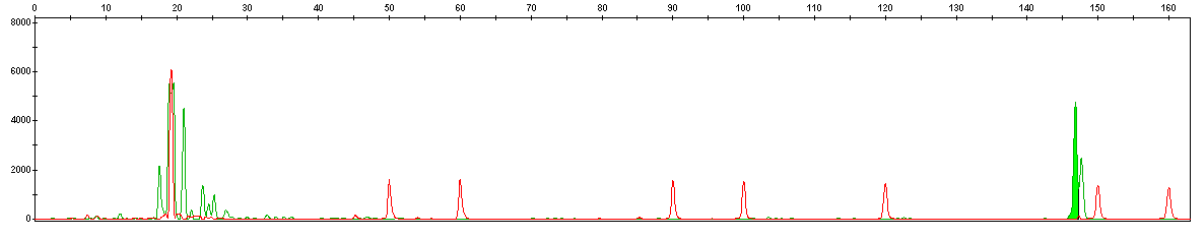

Exon 12

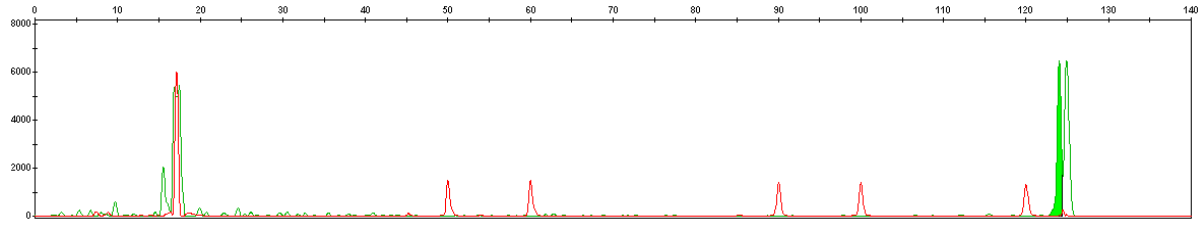
0
10
20
30
40
50
60
70
80
90
100
110
120
130
140
8000
6000
4000
2000
0

Auteursrechtelijke overeenkomst

Ik/wij verlenen het wereldwijde auteursrecht voor de ingediende eindverhandeling:
Heat-transfer resistance based biosensor to detect mutation in patients with PKU

Richting: **master in de biomedische wetenschappen-bio-elektronica en nanotechnologie**
Jaar: **2013**

in alle mogelijke mediaformaten, - bestaande en in de toekomst te ontwikkelen - , aan de Universiteit Hasselt.

Niet tegenstaand deze toekenning van het auteursrecht aan de Universiteit Hasselt behoud ik als auteur het recht om de eindverhandeling, - in zijn geheel of gedeeltelijk -, vrij te reproduceren, (her)publiceren of distribueren zonder de toelating te moeten verkrijgen van de Universiteit Hasselt.

Ik bevestig dat de eindverhandeling mijn origineel werk is, en dat ik het recht heb om de rechten te verlenen die in deze overeenkomst worden beschreven. Ik verklaar tevens dat de eindverhandeling, naar mijn weten, het auteursrecht van anderen niet overtreedt.

Ik verklaar tevens dat ik voor het materiaal in de eindverhandeling dat beschermd wordt door het auteursrecht, de nodige toelatingen heb verkregen zodat ik deze ook aan de Universiteit Hasselt kan overdragen en dat dit duidelijk in de tekst en inhoud van de eindverhandeling werd genotificeerd.

Universiteit Hasselt zal mij als auteur(s) van de eindverhandeling identificeren en zal geen wijzigingen aanbrengen aan de eindverhandeling, uitgezonderd deze toegelaten door deze overeenkomst.

Voor akkoord,

Ramiya Ramesh Babu, Heman Kumar

Datum: **28/06/2013**